An Early-Season Coastal Storm: Conceptual Success and Model Failure

LANCE F. BOSART

Department of Atmospheric Science, State University of New York at Albany, Albany, New York

FREDERICK SANDERS

9 Flint Street, Marblehead, Massachusetts

(Manuscript received 26 October 1990, in final form 8 April 1991)

ABSTRACT

An unusual early-season snowstorm dumped more than 50 cm of snow over portions of interior eastern New York and western New England on 4 October 1987. This was associated with poorly forecasted cyclogenesis. In the wake of atmospheric cooling associated with upward motion and cold advection, additional cooling associated with melting snow in a heavy precipitation region aided in the creation of a low-level dome of cold air to the west of the surface cyclone track. This allowed heavy snow to fall at low elevations. The absence of low-level warm-air advection over the snow region was crucial to the maintenance of the cold dome as relatively warm maritime air to the east was prevented from reaching the area, eroding the cold dome and changing the snow to rain.

The storm was also noteworthy because its development was in accordance with well-known qualitative quasi-geostrophic principles, but the NMC operational prediction models, while simulating the 500-mb circulation well, failed to predict accurately the storm development off the mid-Atlantic coast and its associated precipitation. An investigation of the Regional Analysis and Forecast System (RAFS) initialized fields revealed a critical underestimate of the vertically integrated moisture and lower-troposphere vorticity and divergence in the coastal baroclinic zone of the incipient storm environment at 1200 UTC 3 October 1987. Despite plentiful forcing aloft, the RAFS was never able to simulate the surface development successfully with the improperly analyzed low-level wind field and vertically integrated moisture field.

1. Introduction

On 4 October 1987, an unprecedented early-season snowstorm dumped upward of 50 cm of snow on interior eastern New York and western New England. At sea, gale-force winds developed suddenly along the coast and offshore. Property damage was extensive, and power outages lasting up to one week were widespread, as trees, still in full leaf, toppled on to power lines, homes, and cars. Storm-related deaths totaled 20 people, with more than 300 injuries in the region. A description of this storm can be found in Gedzelman and Lewis (1990) who classified this and other storms as "warm snowstorms" on the basis of the prevalence of above freezing temperatures throughout the lower troposphere during the prestorm period.

Operational guidance on this storm from the National Meteorological Center (NMC), Regional Analysis and Forecast System (RAFS; Hoke et al. 1989), Limited-area Fine-mesh Model (LFM; Gerrity 1977), and Medium Range Forecast Model (MRF; Sela 1980; Caplan et al. 1989; Kanamitsu 1989) as to precipitation type and intensity, and storm track and intensity was woeful. Our interest in this case was prompted by two factors. First, the cyclone development and evolution followed well-known qualitative quasigeostrophic principles, which made the model failures especially puzzling. Second, both authors were personally involved in the storm. The first author was stranded in the Berkshire Hills of western Massachusetts on a trip from Boston, Massachusetts (BOS), to Albany, New York (ALB). (Places mentioned in the text are indicated in Fig. 1, along with simplified terrain.) He recorded heavy, blowing snow (wind gusting over 25 m s^{-1}, snow depths of 40 cm determined by inking his bare arm and measuring the various lengths later) amidst the eerie sound of cracking and falling tree limbs still in full leaf. The second author encountered the storm aboard his sailing craft, the IRV (inadvertent research vessel) *Stillwater,* off the New Jersey coast. The entry in his log for the period 0400–0600 UTC 4 October 1987 when the *Stillwater* was located near 38.6°N,74.2°W tells the story: "Blowing hard. Many rain showers. Cold. Wretched. Gusts to 50 kts".

The purpose of this paper is to document the evolution of the storm, explore possible reasons for the failure of the NMC models to simulate the storm and

Corresponding author address: Dr. Lance F. Bosart, Dept. of Atmospheric Science, State University of New York, at Albany, Albany, NY 12222.

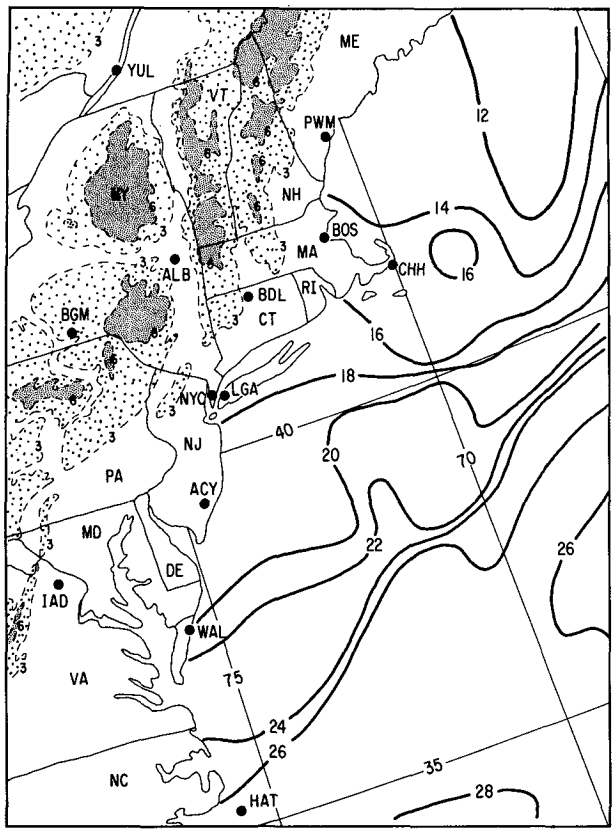

FIG. 1. Simplified terrain map (elevations of 300–600 m and >600 m are shown dotted and stippled, respectively) with conventional three-letter station identifiers and composite sea surface temperature analysis (°C) for 3–4 October 1987.

its associated precipitation shield properly, and to point out the important role of atmospheric cooling by melting snow in preconditioning the lower atmosphere for heavy snowfall. Ludlum (1966, 1968) has indicated that heavy early-season snowfall events in the interior northeastern part of the United States are extremely rare, notable examples having occurred in October 1836 (an even bigger event) and 1925. McGuire and Penn (1953) described an early April snowstorm event in the BOS area in which heavy rain turned to heavy snow, while to the north and south, where the precipitation intensity was lighter, only rain was reported. In effect, the storm made its own cold air beneath the most intense updrafts, and as shown by Wexler et al. (1954), atmospheric cooling by melting snow contributed to the changeover from rain to snow at the surface. Homan and Uccellini (1987) used a sequence of 3-h soundings to show that the changeover from rain-to-sleet-to-snow can occur abruptly in association with cooling from melting snow.

The microphysical aspects of the melting process in stratiform precipitation regions and their possible role in forcing mesoscale circulations near the rain–snow boundary has been explored in a series of papers by Matsuo and Sasyo (1981a,b,c), Stewart (1984, 1985), Stewart et al. (1984), Lin and Stewart (1986), Stewart and King (1987a,b), and Szeto et al. (1988a,b). One outcome of this research is that the deepest radar echoes and clouds occurred close to the surface rain–snow boundary and appeared to mark the signature of a mesoscale circulation driven by melting snow. Modeling studies have further suggested that the observed increase in precipitation intensity near the rain–snow boundary may potentially be attributed to a thermally indirect circulation driven by differential diabatic heating across the melting zone.

Although a number of these microphysical processes were likely operative in the 4 October 1987 snowstorm event, we lack the direct evidence to prove or refute it because of data limitations. For example, no film was available from the 5-cm local-warning radar at the National Weather Service (NWS) Forecast Office in ALB. Similarly, the precipitation echo coverage from the Binghamton (BGM) and New York, New York (NYC), NWS network 10-cm radars was inadequate because of distance limitations to distinguish snowfall intensity variations in the core of the precipitation shield containing the rain–snow boundary. Instead, we will infer evidence for the effect of atmospheric cooling by melting snow through indirect means.

2. Storm overview

The composite sea surface temperature (SST) analysis shown in Fig. 1 was constructed from all available ship observations for the 3–4 October 1987 period. The position of the 20°C SST isotherm is very close to its expected maximum northward climatological location at this time of the year. Sea surface temperatures during the month were 1°–2°C above normal just offshore from Virginia to Cape Cod (NOAA 1987).

Figures 2a and 2b display the total precipitation and snowfall for the 3–4 October period. Precipitation in excess of 20 mm is widespread, and orographic precipitation enhancement can be seen across the eastern Catskill Mountains of New York, the Berkshire Hills of Massachusetts, and the southern Green Mountains of Vermont, where in excess of 100 mm of precipitation is reported. Although the snowfall distribution contains the expected maxima at higher elevations, there are considerable accumulations (10–20 cm) in the mid-Hudson Valley, within the band of heaviest precipitation. In general, however, the snowfall region is confined to the western half of the precipitation shield, a characteristic of many storms.

Manually prepared and analyzed surface sectional maps at 6-h intervals for the period 1200 UTC 3 October–1200 UTC 4 October are shown in Figs. 3 and 4. The principal feature of interest is the coastal trough that extends from western Long Island southward into eastern North Carolina at 1200 UTC 3 October (Fig. 3a). This feature is marked by a prominent wind shift

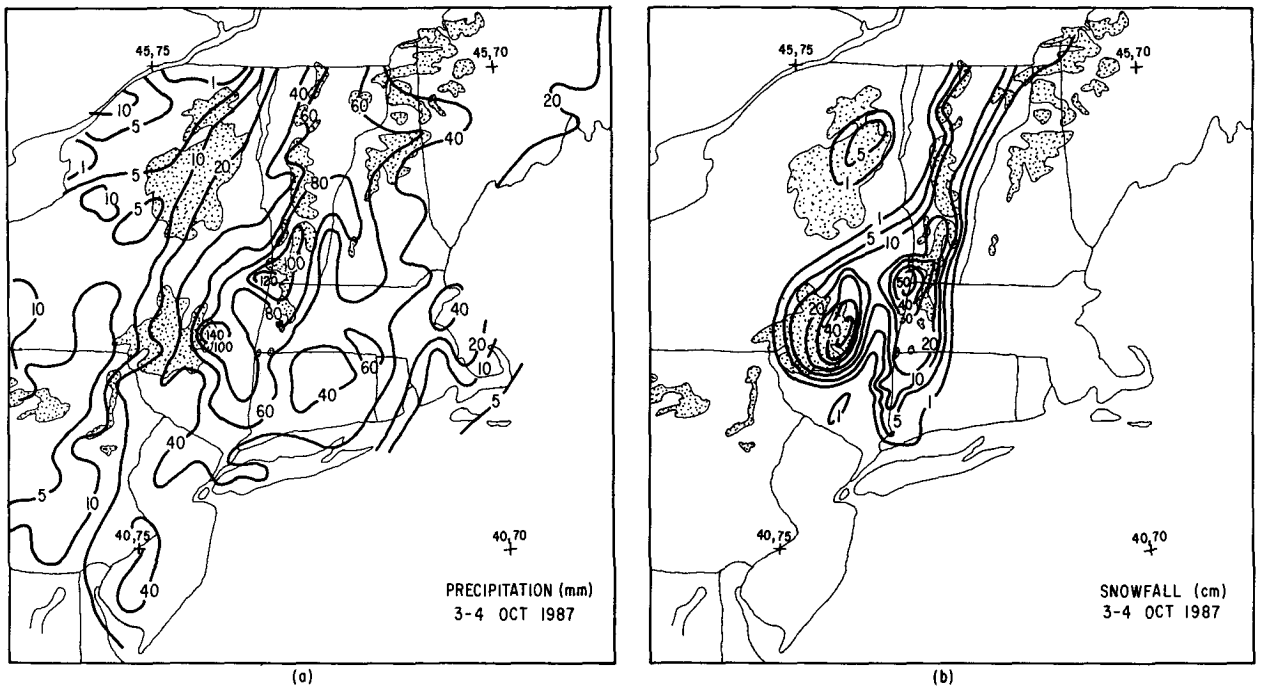

FIG. 2. (a) Accumulated precipitation (left, mm), and (b) snowfall (right, cm) for 3–4 October 1987. Stippling (more smoothed than Fig. 1) denotes elevations >600 m.

to the north and northwest across a modest baroclinic zone with a tighter pressure gradient in the cold air. Weak cyclonic vorticity maxima are estimated to be located over the southern New Jersey coastal waters and just south of Long Island on the basis of the observed winds. An additional feature of interest is the offshore frontal boundary and modest cyclone center (~1010 mb) east of North Carolina. With the +4°C isotherm still west of the St. Lawrence Valley in a region of clearing skies, a forecaster can be forgiven for not considering the likelihood of a major snowstorm.

Subsequently, the coastal trough moves offshore and cyclogenesis commences, weakly at 1800 UTC 3 October (Fig. 3b) and more prominently at 0000 UTC 4 October (Fig. 3c). The initial track of the circulation maximum and then of the cyclone center is southeastward, which is analogous to the motion of a lee cyclone east of the Rockies, except there are no mountains in coastal New Jersey and the Delmarva Peninsula. As more rapid deepening begins, the cyclone turns eastward and then northeastward, eventually passing just west of BOS at 1200 UTC 4 October (Figs. 3c, 3d, and 4). Meanwhile, the weak cyclone to the east continues northward, links up with the developing warm front circulation east of Cape Cod at 0600 UTC, and is totally absorbed into the intensifying cyclonic circulation by 1200 UTC 4 October. The storm deepens from 1004 to 990 mb in the 12-h period ending 1200 UTC 4 October, and 23 mb in the 24-h period ending the same time, rendering it a borderline moderate bomb according to the criteria established by Sanders and Gyakum (1980). Note that the first appearance of surface temperatures below 0°C can be seen at 0600 UTC 4 October over the higher elevations (>600 m) of northwestern Pennsylvania. No frozen precipitation is reported anywhere at this time. By 1200 UTC 4 October, an area of 0°C or lower surface temperatures marks the snow region centered over lower elevations of the mid-Hudson Valley. There is no evidence to indicate that this cold pocket was created by horizontal advection processes.

The corresponding manually prepared and analyzed 850-mb and 500-mb maps for the 24-h period ending 1200 UTC 4 October are shown in Fig. 5. Cyclogenesis, associated with the approach of a dome of cold air (upper-level trough containing uplifted isentropic surfaces) at 500 mb from the Ohio Valley, is initiated along the 850-mb coastal baroclinic zone. As the 500-mb system turns northeastward on approaching the coast, the cold dome weakens, the lowest reported temperature increasing from −28° to −22°C. At 850 mb, the axis of coldest air is drawn southward across western Pennsylvania and New York into the periphery of the intensifying circulation. The most noteworthy feature at 850 mb is the strong band of warm-air advection across central New England at 0000 and 1200 UTC 4 October that marks the eastern and central portion of the heavy precipitation shield. Geostrophic frontogenesis at 850 mb north of the low center is indicated at 0000 UTC, consistent with the highly ageo-

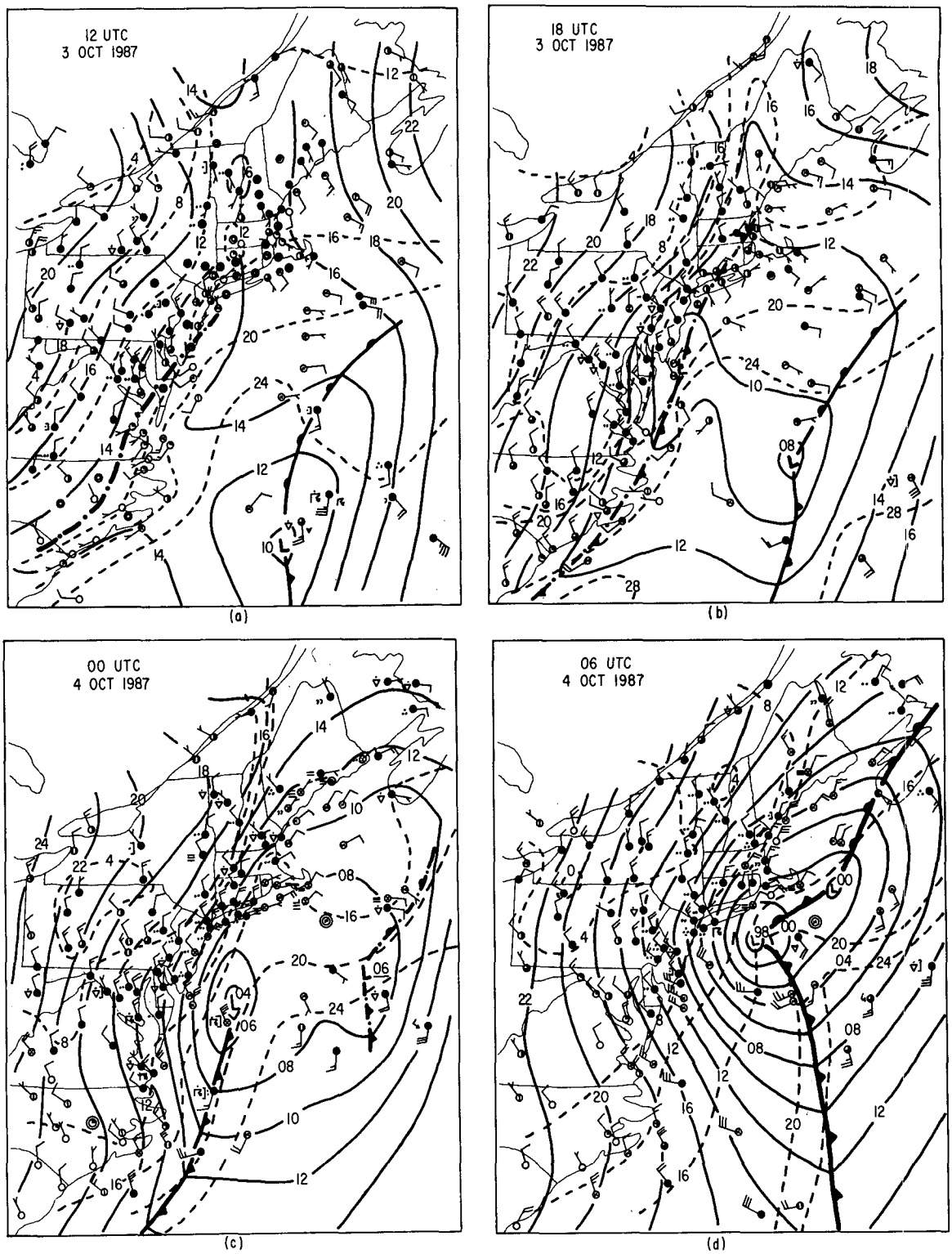

FIG. 3. Surface sectional maps of mean sea level pressure (solid) every 1 mb and temperature (dashed) every 4°C with conventional frontal boundaries, weather symbols and station model for: (a) 1200 UTC 3 October 1987, (b) 1800 UTC 3 October 1987, (c) 0000 UTC 4 October 1987, and (d) 0600 UTC 4 October 1987. Winds plotted according to convention with each pennant, full barb, and half barb denoting 25, 5, and 2.5 m s^{-1}, respectively. Cyclone center is denoted by "L" symbol.

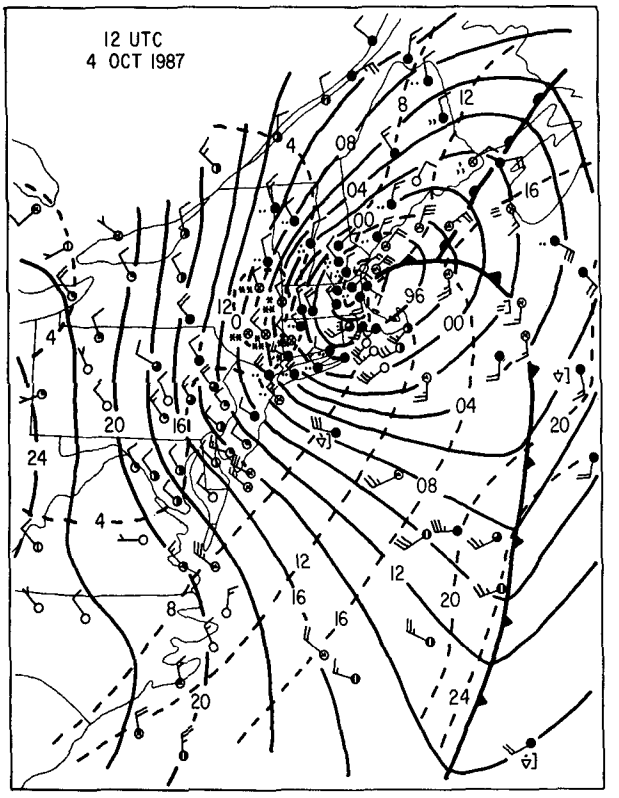

FIG. 4. As in Fig. 3 except for 1200 UTC 4 October 1987.

strophic wind at ALB. Near-neutral thermal advection is indicated over the mid-Hudson Valley in the core of the snow area.

Figure 6 shows an analysis of the 1000–500-mb thickness and superposed 500-mb absolute vorticity for the 14-h period ending 1200 UTC 4 October. The individual analyses were traced directly from the initialized RAFS fields. The frontal positions were transcribed from the surface analyses. The key point is that cyclogenesis is initiated as an area of cyclonic vorticity advection by the thermal wind that overspreads the coastal baroclinic zone. During the more rapid intensification stage, there is appreciable cyclonic vorticity advection by the thermal wind over the cyclone center. This cyclonic development follows principles first established by Sutcliffe (1947) and is presented in terms of modern quasigeostrophic theory by, e.g., Trenberth (1978) and Holton (1979). It is surprising, therefore, that the operational prediction models failed to simulate this cyclogenesis, as will be demonstrated in section 5.

3. Vertical structure

Figure 7a presents soundings for Sterling, Virginia (IAD), and Atlantic City, New Jersey (ACY), at 1200 UTC 3 October. These stations straddle the coastal baroclinic zone shown in Fig. 3a. Comparison with Fig. 5a reveals the existence of a westward tilting trough characterized by a near equivalent barotropic structure (minimal directional shear above 700 mb at both IAD and ACY) in the middle troposphere. Modest baroclinity is present throughout the lower half of the troposphere between IAD and ACY. The moist conditions at IAD combined with a jet in excess of 50 m s^{-1} at 250 mb and the approach on an area of cyclonic vorticity advection by the thermal wind (Fig. 6a) supports the idea of eventual cyclogenesis in the vicinity of New Jersey, as is observed.

The 0000 and 1200 UTC 4 October soundings for ALB are shown in Fig. 7b (the 1200 UTC sounding was launched in heavy, wet snow and terminated at 581 mb). Appreciable overnight cooling occurred below 800 mb, 12 h after the onset of heavier precipitation (Fig. 9) in the presence of geostrophic warm-air advection, but with ageostrophic cold-air advection at 850 mb (Figs. 5e and 5f). Note, from Figs. 5d–f, the growth in 850-mb temperature contrast in the ALB region and eastward by 1200 UTC 4 October. This occurs in the presence of the aforementioned geostrophic frontogenesis, which maximizes at 0000 UTC 4 October. It is possible that the maximum 850-mb cooling to near −5°C at ALB at 1200 UTC 4 October may be a manifestation of the ageostrophic transport of cold air from near Maniwaki, Quebec (71722), where it was −7.1°C at 0000 UTC 4 October. The southeastward expansion of the 0° and −4°C isotherms during this period, where radiative cooling probably was not significant, is additional indirect evidence for this assertion.

At ALB, one 0°C isothermal layer is found between 750 and 700 mb with a second such layer (~200–300 m thick) just below 950 mb at 1200 UTC 4 October. The latter isothermal layer is likely produced by melting snow in a saturated environment, as will be discussed later. An upward extrapolation of the 1200 UTC 4 October ALB sounding to 500 mb along a moist adiabat yields geopotential height and temperature values of 549 dam and −19°C, respectively, which are plotted in Fig. 5c. The corresponding 1000–500-mb thickness at ALB is computed to be 543 dam, somewhat above the 540-dam climatological thickness value for rain versus snow in this region. Evidently, the early date in the snow season has the most to do with the "surprise" for this event.

It is remarkable that so much snow can fall near sea level (the elevation of the Albany County airport is 88 m) so early in the season with a comparatively warm 1000–500-mb thickness. The presence of low-level cold air and the absence of any corresponding marine-air fetch is apparently crucial in creating an environment in which the 0°C isothermal layer associated with melting snow can reach the surface. This point is made more firmly in Fig. 8, which shows the 1200 UTC 4 October soundings for ALB and Portland, Maine

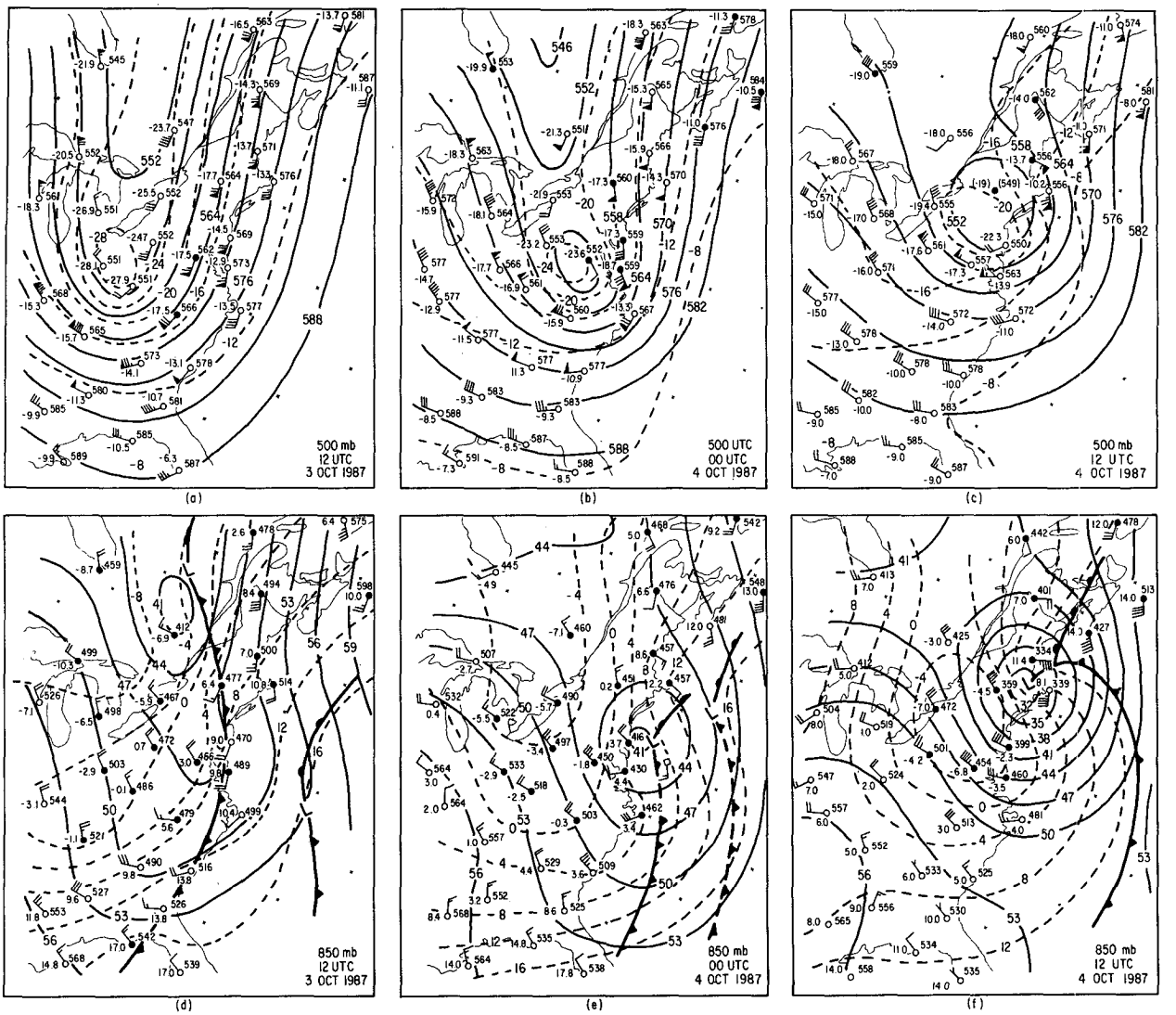

FIG. 5. Geopotential height (solid, dam) and temperature (dashed, °C) at 500 mb (top) and 850 mb (bottom) for: (a), (d) 1200 UTC 3 October 1987; (b), (e) 0000 UTC 4 October 1987; and (c), (f) 1200 UTC 4 October 1987. Height contours every 6 dam (3 dam) at 500 mb (850 mb); isotherms every 4°C. Winds as in Fig. 3. Solid circles denote a temperature–dewpoint temperature spread of ≤5°C.

(PWM). A deep layer of veering winds, indicative of warm advection, culminates in a 60 m s^{-1} southerly jet above 300 mb at PWM. A well-defined warm-frontal inversion is found in the 950–850-mb layer above a surface moist-adiabatic mixed layer. Although PWM is in the cold air, the baroclinity below 700 mb between ALB and PWM is very large. The difference is that the airflow at PWM has a marine trajectory with water temperatures in the Gulf of Maine in the 12°–13°C range (Fig. 1). Thus, the confluence of a continental and marine airstream across central New England contributes to the creation of a very strong low-level baroclinic zone and sets the stage for a deep layer of warm-air advection above the low-level cold dome. Ascent is then implied above the cold dome with the approach of an area of cyclonic vorticity advection by the thermal wind (Fig. 6c) and the presumed thermally direct ageostrophic circulation associated with geostrophic frontogenesis (Fig. 5e), the latter effect is not included in the simple Trenberth (1978) theory.

4. Evidence for atmospheric cooling due to melting snow

Figure 9 shows a time section of various meteorological parameters at ALB as gleaned from the NWS surface observations for the period 0600 UTC 3 October through 2000 UTC 4 October. A weak trough line passes the ALB area in the vicinity of 1200 UTC 3 October (Fig. 3a) accompanied by a period of light rain (peak hourly amount of ~3 mm near 0900 UTC) and a slow pressure increase amounting to ~4 mb by

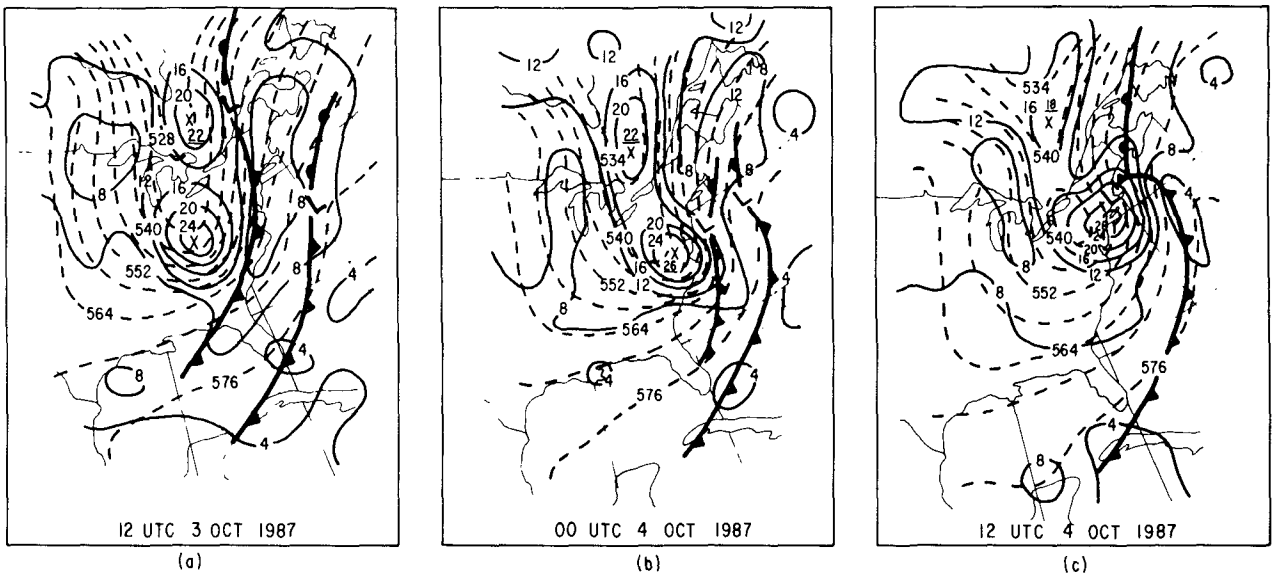

FIG. 6. Absolute vorticity (solid) every 4×10^{-5} s^{-1} at 500 mb and 1000–500-mb thickness (dashed) every 6 dam for: (a) 1200 UTC 3 October 1987, (b) 0000 UTC 4 October 1987, and (c) 1200 UTC 4 October 1987.

1600 UTC 3 October. The modest nature of the trough is illustrated by the 6-h period of calm winds sandwiched between southeasterlies and northwesterlies. After an initial temperature decrease to the wet-bulb temperature of ~11°–12°C with the onset of precipitation, the temperature holds steady until the start of northwesterly flow and cold-air advection after 1500 UTC 3 October. Precipitation intensity picks up again after 2200 UTC 3 October, averaging 1–2 mm h^{-1} by 0600 UTC 4 October. This latter increase is accompanied by a strengthening northerly flow, an additional temperature decrease to ~2°C, and the onset of in-

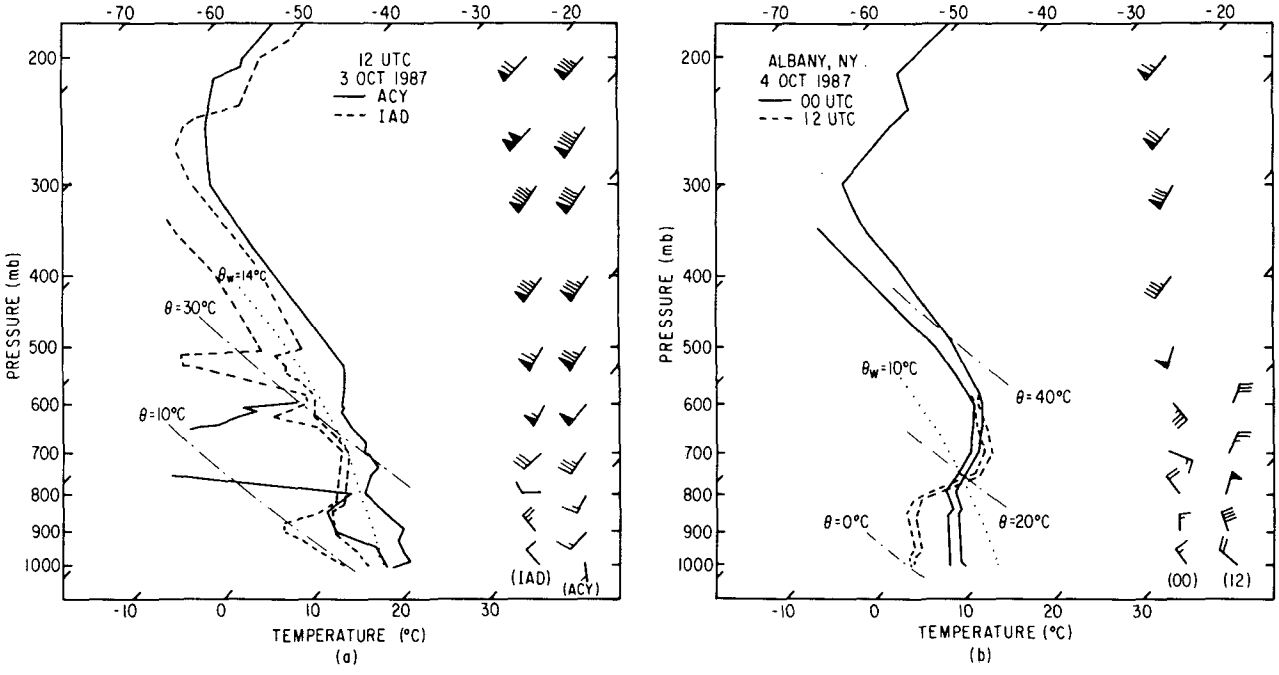

FIG. 7. Skew T–log p format soundings for Sterling, Virginia (72403, IAD, solid), and Atlantic City, New Jersey (72407, ACY, dashed), for 1200 UTC 3 October 1987 (left); Albany, New York (ALB, 72518), for 0000 UTC (solid) and 1200 UTC (dashed) 4 October 1987 (right). Winds as in Fig. 5.

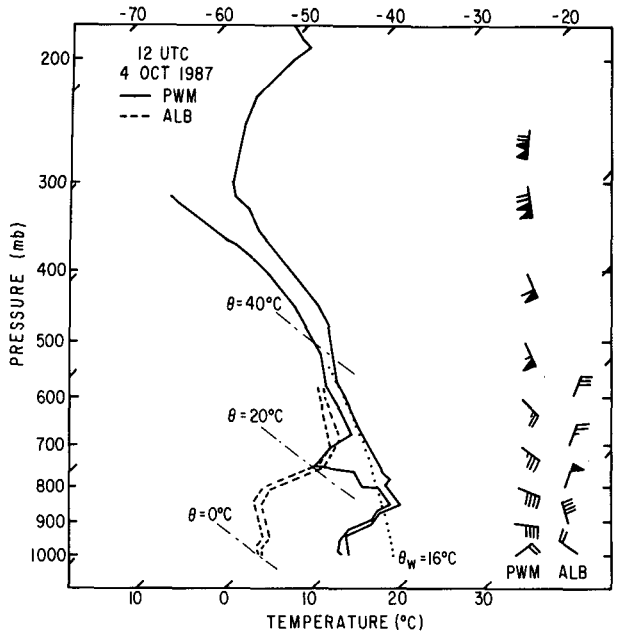

FIG. 8. As in Fig. 7 expect for Portland, Maine (72606, PWM, solid), and Albany, New York (72518, ALB, dashed), at 1200 UTC 4 October 1987.

termittent ice pellets and a few wet snowflakes mixed in with the rain. The changeover to snow is complete by 1300 UTC 4 October following a period of 4–6 mm h^{-1} average precipitation rate as the temperature reaches close to 0°C. Subsequently, it snowed very hard with a couple of peals of thunder with a precipitation intensity of 8–10 mm h^{-1} for 5 h (equivalent to an hourly snowfall rate of 7–10 cm at the standard 10:1 water-equivalent ratio). The official reports of "light" snow, aside from the 1300 UTC observation of heavy snow, are misleading, given the observed precipitation intensity and the local whiteout conditions.

Support for the existence of an isothermal layer near 0°C in the snow region is presented in Fig. 10, which shows minimum temperature as a function of elevation for 74 locations gleaned from a local network of cooperative weather observers and data published in NOAA's monthly climatological bulletin for New York and New England. The assumption was made that the minimum temperature coincided with the time of significant snowfall based on the NWS observations from ALB and the independent records of local cooperative observers (not shown). An inspection of Fig. 10 discloses an envelope of minimum temperatures within ~±1°C of freezing for the 73 stations ranging in elevation from just above sea level to just above 800 m. The lone exception is the −4.3°C minimum temperature at Mount Mansfield, Vermont (just under 1200 m elevation), which probably represents conditions in the wedge of cold air centered near 850 mb just above the lower-level isothermal layer (Fig. 8). We thus conclude that there is reasonably good indirect evidence for the importance of atmospheric cooling (saturation

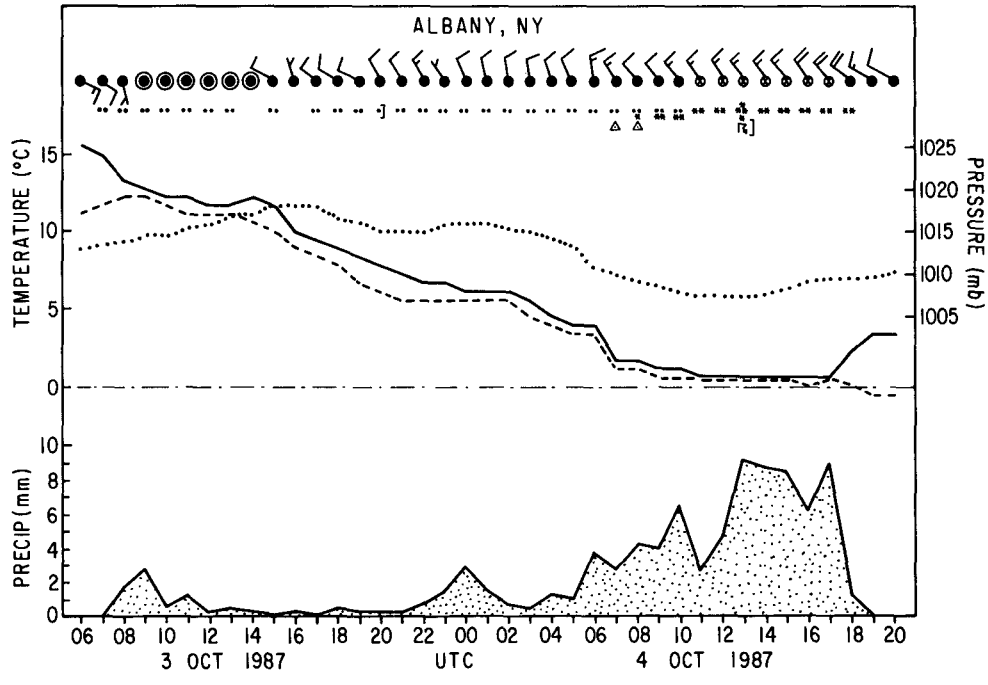

FIG. 9. Albany, New York, time series of winds, present weather, sea level pressure (dotted, mb), surface temperature (solid, °C), dewpoint temperature (dashed, °C), and hourly precipitation (stippled, mm) from 0600 UTC 3 October 1987 through 2000 UTC 4 October 1987. Thin horizontal dash-dot line denotes 0°C isotherm.

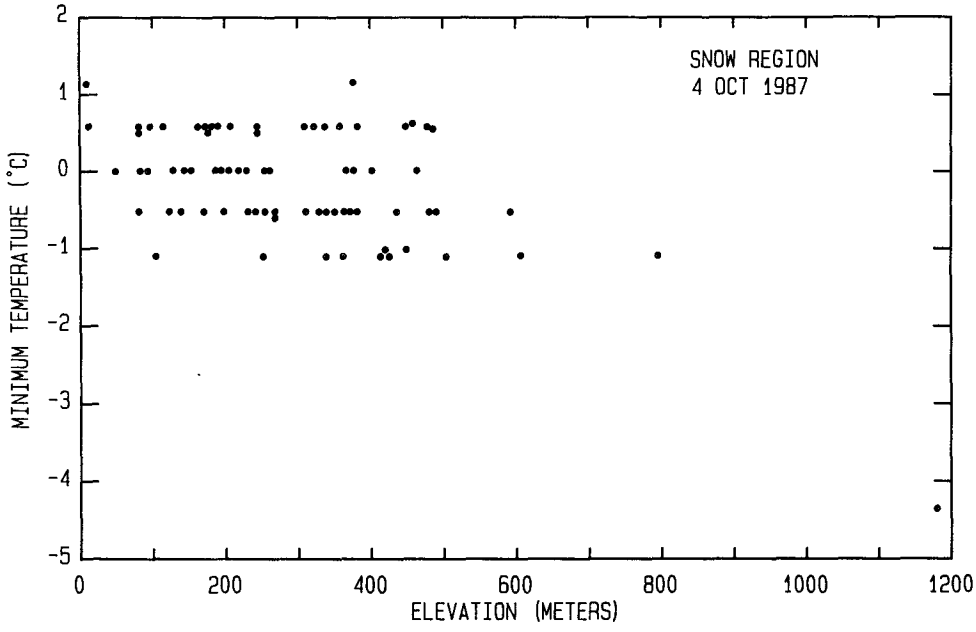

FIG. 10. Minimum temperature (°C) versus elevation (m) within the snow region on 4 October 1987.

implies ascent and ascent implies cooling) due to melting snow in the present case.

Given a knowledge of the observed precipitation rate and the assumption of saturated air, we can ask the question of how long will it take to develop a 0°C isothermal layer and how deep will it be. To first approximation the temperature changes due to adiabatic cooling and horizontal advection will be neglected. The heat balance equation after Wexler et al. (1954) can then be written as:

$$c_p \frac{\Delta p}{g} \Delta T + L_c \frac{\Delta p}{g} \Delta q = L_f m, \qquad (1)$$

where $\Delta p/g$ is the mass per unit area, m is amount of ice (snow) melting in a layer of thickness Δp, ΔT is the mean cooling of the layer, Δq is the mean specific-humidity change of the layer, and L_c, L_f are the latent heats of condensation and fusion, respectively.

From a skew T–log p adiabatic chart, for saturated air near 0°C with a pressure of 1000 mb we can approximate

$$\Delta q \sim 0.3 \times 10^{-3}\ \mathrm{K}^{-1}\ \Delta T, \qquad (2)$$

so that the approximate heat balance equation becomes:

$$(c_p + 0.3 \times 10^{-3}\ \mathrm{K}^{-1}\ L_c)(\Delta p/g)\Delta T = L_f m. \qquad (3)$$

For a 5 mm h^{-1} equivalent precipitation rate, (3) can be solved to yield:

$$\Delta T \sim 1.0°\mathrm{C\ h}^{-1}\ (100\ \mathrm{mb})^{-1}. \qquad (4)$$

According to Fig. 9, in the 0600–1200 UTC 4 October period, when rain mixed with ice pellets and snow, and gradually changed over to snow, the hourly precipitation rate averaged 3–5 mm h^{-1}; therefore, the calculated hourly cooling rate for a 100-mb-thick layer from (4) based on a 5 mm h^{-1} precipitation rate is qualitatively reasonable. Caution must be exercised, however, because inspection of the ALB soundings in Fig. 8 suggests that adiabatic cooling (saturation implies ascent, and ascent implies cooling) and cold advection also contributed to the evolution of the thermal structure. Given that the lower troposphere was saturated over the mid-Hudson Valley at 0000 UTC 4 October (Fig. 8), it is unlikely that evaporation of precipitation contributed significantly to cooling. We conclude that the generation of a nonadvective cold pool at the surface is at least plausible.

5. Model comparisons

The purpose of this section is to document the performance of the NMC operational RAFS (and to a lesser extent the MRF) prediction model for this event. [Note that the Nested Grid Model (NGM) is the cornerstone of RAFS.] Cyclone locations and central pressures, as gleaned from an average of the authors' individual manual analyses, the manually prepared Northern Hemisphere (NH) analyses at NMC, the NMC front hemisphere automated analyses (FH), and the initialized RAFS analyses are shown in Fig. 11a for the period 1200 UTC 3 October through 1200 UTC 4 October. Two conclusions are obvious from an inspection of Fig. 11a. First, the manual analyses agree

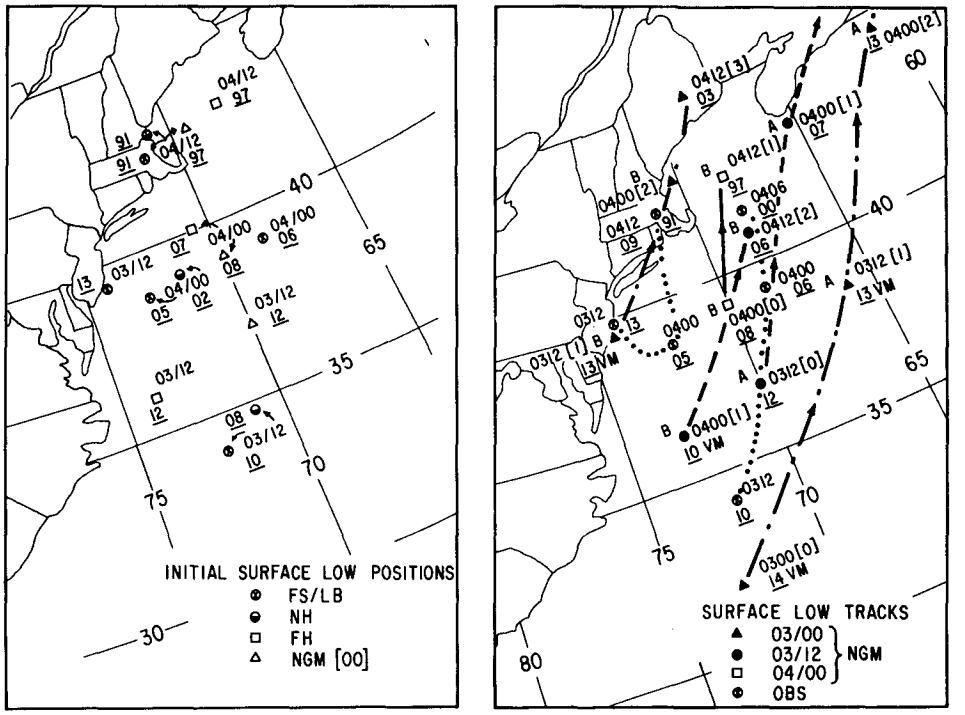

FIG. 11. (a) Analyzed surface cyclone positions from the Sanders–Bosart subjective analyses, ⊗; the NMC subjective Northern Hemisphere analyses, ⊖; the NMC objective front hemisphere analyses, □; and the initialized RAFS Nested Grid Model (NGM) analyses, △ [00] according to (day/UTC). Underlined two-digit number is the cyclone central pressure (mb), leading 9 or 10 omitted; (b) surface cyclone tracks as determined from the Sanders–Bosart subjective analyses (⊗, dotted), and the RAFS–NGM forecast runs initialized 0000 UTC 3 October 1987 (▲, dash–dot), 1200 UTC 3 October 1987 (●, dashed), and 0000 UTC 4 October 1987 (□, solid). VM denotes vorticity maximum. All other plotting conventions as in (a). Two cyclone paths (A, B) are shown.

fairly well on cyclone position and intensity, except for the initial periods of 1200 UTC and 1800 UTC 3 October (not shown) when the advantage of the research mode, as opposed to the time-constrained operational mode, permitted a more careful analysis. Second, the automated FH and initialized RAFS analyses could not locate either observed cyclone at 1200 UTC 3 October, with the former preferring an intermediate position and the latter well to the east of either observed system. Although the situation was improved at 0000 UTC 4 October, both automated specifications were still 200–300 km too far east and north of the significant cyclone center due south of Long Island. By 1200 UTC 4 October, the RAFS initialized the cyclone 100-km east-northeast of BOS (observed center just west of BOS, recall Fig. 4), while the FH automated analysis placed the cyclone even farther east in the Gulf of Maine. Only by 0000 UTC 5 October, after the storm has ceased to deepen and has begun to fill, do all cyclone positions (including our manual location, not shown) come into reasonable proximity.

The observed cyclone tracks and RAFS forecast storm tracks for runs initialized at 0000 and 1200 UTC 3 October, and 0000 UTC 4 October are shown in Fig. 11b. Observed cyclone A is the weak eastern system (noted in Fig. 3) that eventually becomes absorbed into the main cyclonic circulation. Another weak cyclone located north of the St. Lawrence River valley (Fig. 3a) steadily decays and is absorbed into the circulation of dominant cyclone B, which grows out of a vorticity maximum on the coast of New Jersey at 1200 UTC 3 October. None of the RAFS prognostications could capture cyclone B with the exception of the initialization from 0000 UTC 3 October, which took a much weaker storm rapidly northeast (by more than 12 h too fast) and was operationally useless. A careful comparison of Fig. 11a with 11b leads to the conclusion that the RAFS analysis and initialization procedure results in a significant mislocation of the initial cyclone position.

The above problems also extend to the MRF and LFM (not shown) operational models. Values of central pressure of the cyclone are shown in Fig. 12 for MRF and RAFS analyses and forecasts at a number of ranges. The manually analyzed North American (NA) map central pressures are also included for comparison. Three groupings are apparent at 1200 UTC 4 October: 1) the manual analyses cluster at 991 mb in-

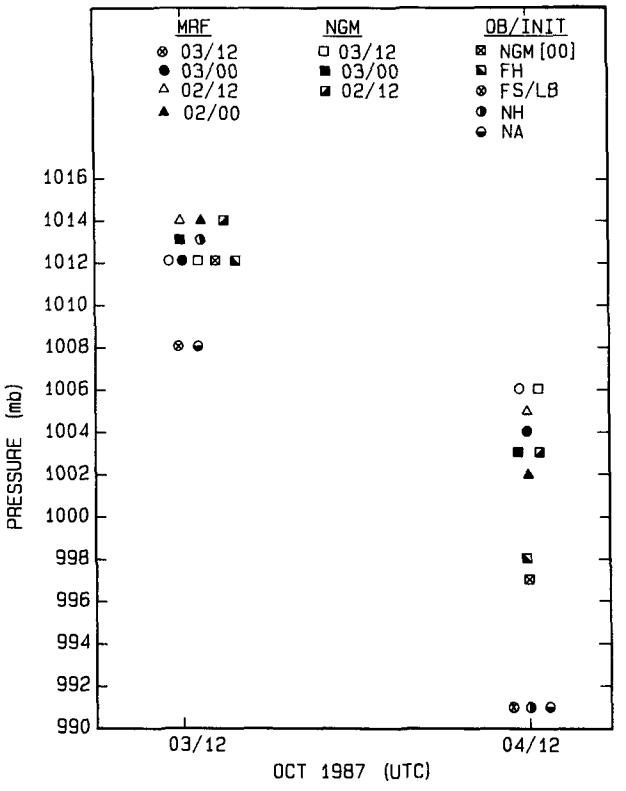

FIG. 12. Cyclone central pressure (mb) verifying 1200 UTC 3 and 4 October 1987 for the various subjective and objective analyses and forecasts initialized according to the convention and times shown at the top of the diagram. Day/time convention as in Fig. 11.

dicative of 17-mb deepening in 24 h, 2) the automated initialized analyses cluster at 997–998 mb indicative of a more modest 14-mb deepening beginning from a higher pressure base 24 h earlier, and 3) the cluster from different forecast projections centered between 1006 and 1002 mb and representative of very modest cyclogenesis. Comparison of Fig. 11 with 12 shows these modest cyclogenesis forecasts to be useless when phase information is considered.

An analysis of the RAFS 500-mb absolute-vorticity and absolute-vorticity advection maxima centers, as determined subjectively from the facsimile charts, are plotted in Fig. 13, along with the initialized and forecast positions of the absolute vorticity centers for different forecast projections. The RAFS initialized surface-low positions (*not* the manually derived locations from Fig. 11a) are also shown for comparison. Two conclusions are immediately apparent. First, cyclogenesis begins as the vorticity center, and associated vorticity advection maximum turns the bottom of the trough and moves northeastward while overtaking the surface cyclone. This indicates that the actual surface cyclone is well behaved from qualitative quasigeostrophic considerations. The observed cyclonic rotation of the position of the 500-mb vorticity center relative to the surface-cyclone position is as expected for deepening cyclones (see, e.g., Sanders 1987a). Second, the position and intensity of the 500-mb vorticity centers are reasonably well forecasted for all projections, particularly at 0000 UTC 5 October when the storm is over. A possible exception is the 48-h forecast 22×10^{-5} s^{-1} absolute-vorticity maximum in extreme southern Pennsylvania at 0000 UTC 4 October. Also, note that the forecast vorticity centers are not deep enough for all forecast projections valid 1200 UTC 3 October.

The corresponding 12-h and 24-h mean sea level pressure and 1000–500-mb thickness forecasts from the RAFS and MRF models are shown in Fig. 14 for 1200 UTC 3 October, the time of incipient cyclogenesis (note that AVN refers to the aviation model, which is identical to the MRF except that it is run from 1200 UTC data with an earlier data cutoff time and only out to 72 h). Comparison with Fig. 3a reveals that the 24-h RAFS and MRF–AVN forecasts overemphasized the northern low along the New York–Quebec border and failed to depict adequately the coastal trough to the south. According to Fig. 3a, a north-northeasterly surface geostrophic flow is indicated from southeastern New York to eastern Virginia at this time. Both the RAFS and MRF–AVN 24-h forecasts (Figs. 14b and 14d), however, show an offshore geostrophic gradient with cold-air advection and no direct threat of coastal cyclogenesis. The 12-h RAFS and MRF–AVN forecasts for 1200 UTC 3 October (Figs. 14a and 14c) correctly show a weaker northern low, but the latter model errs in placing a southern system too far offshore. Meanwhile, the 12-h RAFS forecast (Fig. 14c) finally detects an elongated coastal trough. However, comparison with Fig. 11b reveals that the forecast cyclone, which emerges out of this coastal trough, reaches the vicinity of BOS 12 h too soon and with a central pressure of 1009 mb in comparison to an observed value of 991 mb (Fig. 4).

Cyclogenesis east of New England is shown in Figs. 15a and 15b for the 12- and 24-h forecasts verifying 1200 UTC 4 October. While some precipitation over eastern New England would be expected with this storm track, the forecast storm is still too weak and too far offshore to be a major snowstorm threat for interior eastern New York and extreme western New England. Similarly, the RAFS 24-h forecast verifying 1200 UTC 4 October (Fig. 14d) agrees well with the AVN model in forecasting modest cyclogenesis east of New England. The first hint of a storm track closer to the coast is revealed in the RAFS 12-h forecast of a 997-mb cyclone roughly 150 km northeast of BOS at 1200 UTC 4 October (Fig. 15b). Accumulated forecast precipitation totals through 0000 UTC 5 October with the RAFS run from 0000 UTC 4 October (not shown) remained generally under 20 mm (5 mm) in eastern New England (eastern New York) and were not viewed as a threat for a record-breaking early-season snowstorm when the forecasts became available to the field shortly

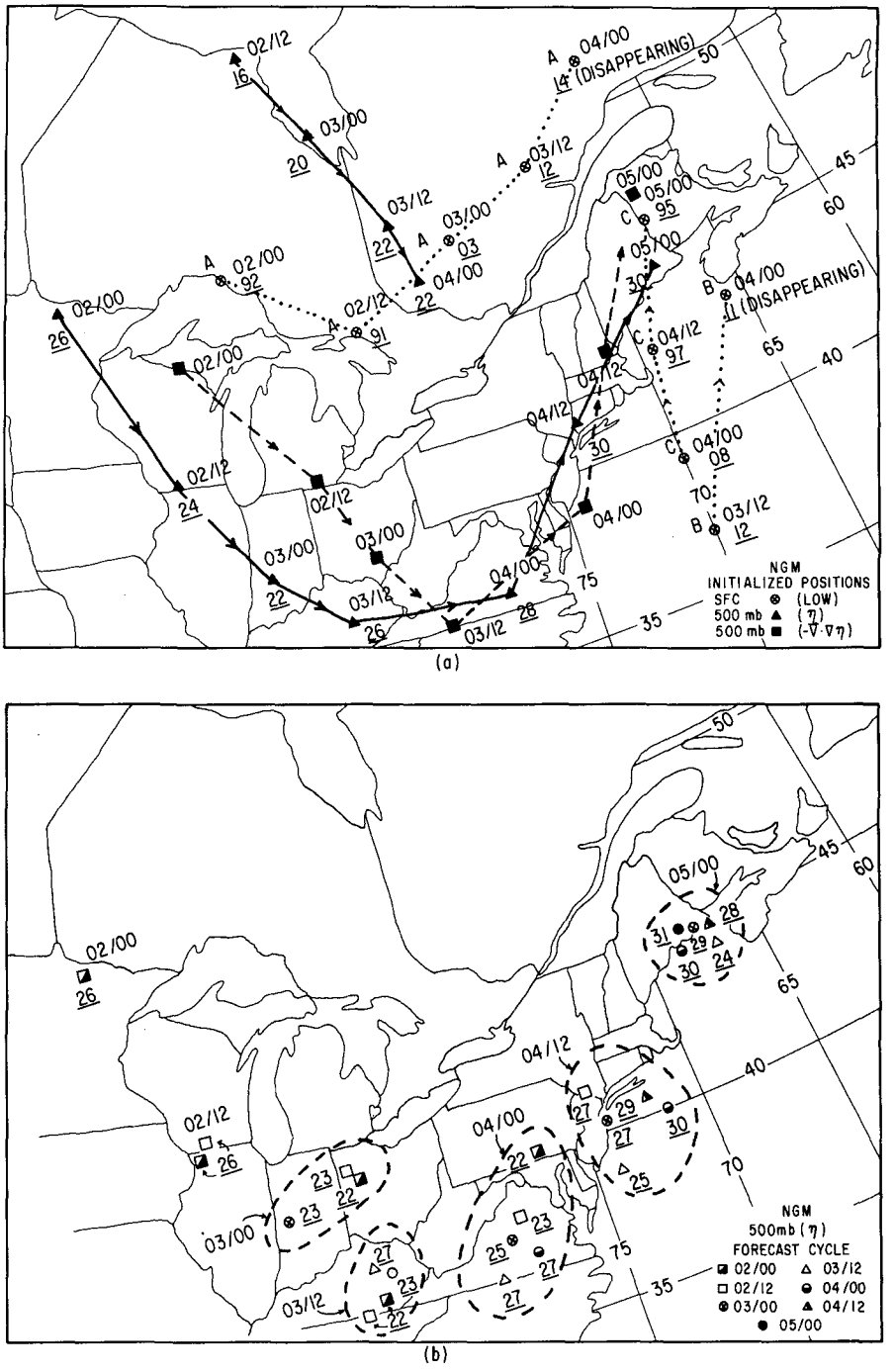

FIG. 13. (a) RAFS–NGM initialized surface cyclone (⊗) and 500-mb absolute-vorticity maximum (▲) locations for days and times plotted according to the convention in Fig. 11. Underlined two-digit number refers to the absolute-vorticity maximum ($\times 10^{-5}$ s^{-1}). Subjectively estimated location of maximum absolute-vorticity advection is given by ■. Tracks are shown by dotted, solid, and dashed lines, respectively. (b) as in (a) except the locations of the initialized and forecast absolute vorticity maxima are plotted according to the convention in the legend. Dashed lines encircle initialized and forecast projections, all verifying the same time.

before midnight, local time, on Saturday 3 October. An unsuspecting public went to bed that evening in blissful ignorance of the whiteout conditions that would greet numerous residents of eastern New York and western New England only 6–8 h later.

Comparison of Figs. 13–15 illustrates that reasonably

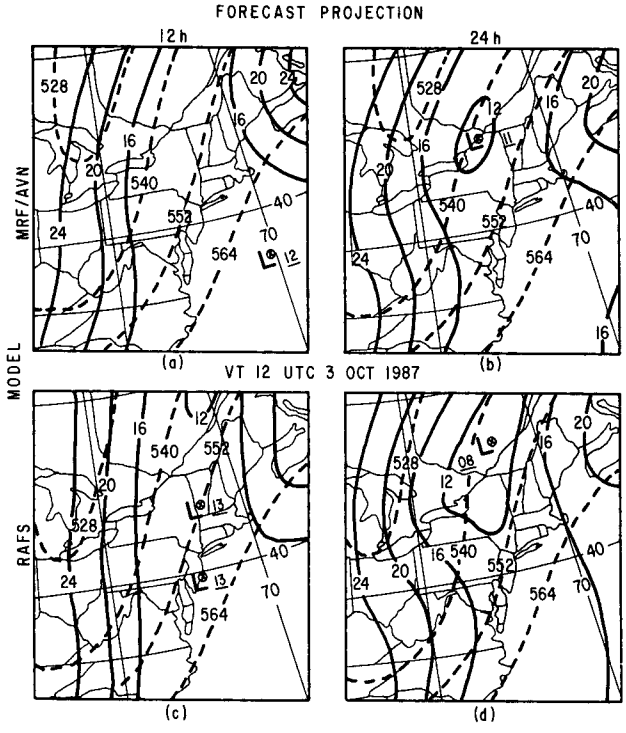

FIG. 14. Mean sea level isobars (solid, every 4 mb) and 1000–500-mb thickness (dashed, every 12 dam) for: (a), (b) 12-h and 24-h MRF–AVN forecasts verifying 1200 UTC 3 October 1987, and (c), (d) 12-h and 24-h RAFS forecasts verifying the same time. Position of cyclone centers (L) marked by ⊗ symbols with underlined central pressure (mb) adjacent.

accurate 500-mb circulation forecasts do not always guarantee accurate surface weather forecasts. This is dramatically illustrated by Fig. 16, which depicts 12-h RAFS accumulated precipitation maps for various forecast projections. Comparison with Fig. 2 shows the model quantitative precipitation forecasts are wretched both in terms of precipitation location and intensity. As an example, the RAFS and LFM (not shown), initialized from 0000 UTC 4 October data, predicted 0.7 and 1.5 mm of equivalent precipitation, respectively, at ALB after 1200 UTC 4 October, but 35–40 mm were observed to actually fall in the region. The corresponding probability of precipitation forecast (POP) from the LFM-based model output statistics (Glahn and Lowry 1972 and Carter et al. 1989) at ALB for the 12-h period ending 0000 UTC 5 October was 20% in the form of rain. Forecasters and citizens alike were equally surprised to wake up the next morning to a whiteout amidst a cacophony of sounds from howling winds, thunder, and crashing tree limbs still in full leaf.

It is also noteworthy that a special RAFS "D-grid" run for this case (not shown) from 0000 UTC 3 October failed to make a significant forecast improvement. [The RAFS system (Hoke et al. 1989) has been coded so that finer-resolution runs are possible; the D-grid resolution is ~40 km]. The 36-h surface forecast verifying 1200 UTC 4 October, for example, placed a 1001-mb low center ~ 100 km east-southeast of PWM after approximately 10–15 cm of predicted precipitation had fallen (and ended) over extreme eastern New York and western New England. Other factors besides improved model horizontal resolution were evidently crucial to a successful forecast in this case.

Motivated by the failure of the operational NMC prediction models to systematically produce a sufficiently intense cyclone close enough to the coast, it was decided that the initial atmospheric conditions available to the models would be examined. The analysis cycle at 0000 or 1200 UTC begins with a forecast for the current model time from the previous model time, which serves as a first guess to the actual objective analysis of the available surface and upper-air observations. Once the analysis is complete, an initialization procedure is invoked to bring the mass and wind field into reasonable balance prior to the integration of the primitive equations used in the model forecast. Accordingly, it was decided that the moisture, thermal, and wind fields would be examined, the results of which follow for the RAFS forecasts.

A manually prepared analysis of the surface to 500-mb mean-layer relative humidity is shown in Fig. 17a for 1200 UTC 3 October along with present weather reports of precipitation. All the plotted data was avail-

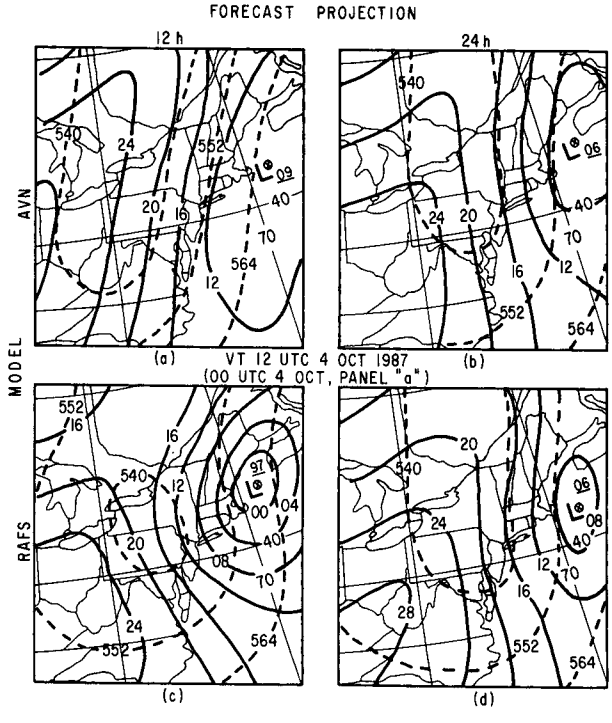

FIG. 15. As in Fig. 14 except for forecasts verifying 1200 UTC 4 October with the exception of panel (a), which shows the AVN forecast for 0000 UTC 4 October 1987.

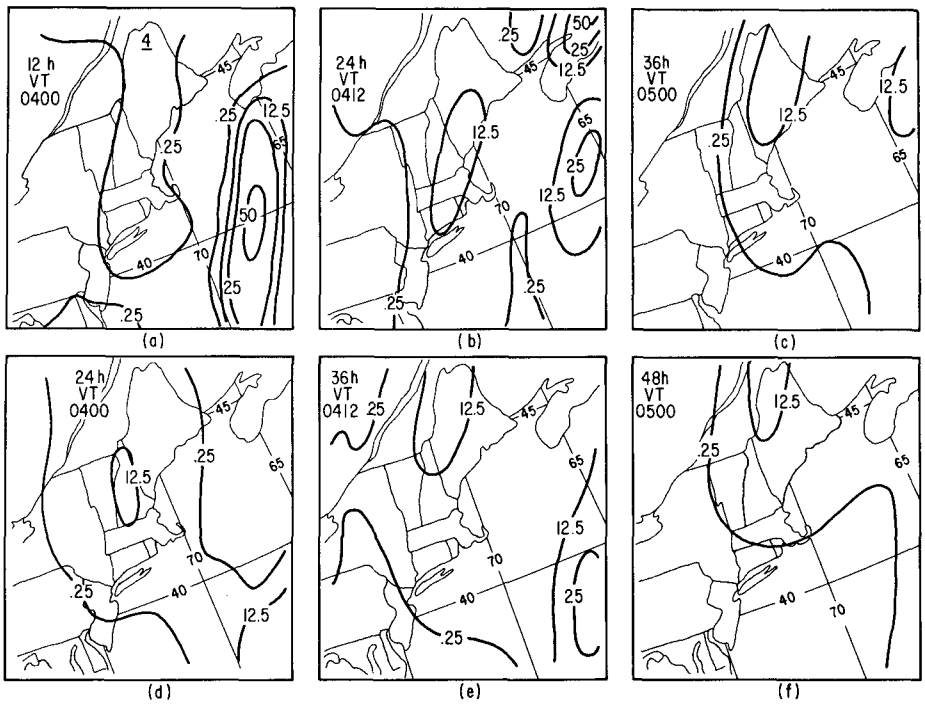

FIG. 16. RAFS accumulated 12-h precipitation (mm) from the 1200 UTC 3 October 1987 (0000 UTC 4 October 1987) forecast cycle at the top (bottom) for periods ending 0000 UTC 4 October 1987 (left), 1200 UTC 4 October 1987 (middle), and 0000 UTC 5 October 1987 (right). Contours are labeled in millimeters.

able to the NMC analysis and initialization packages. Comparison of Figs. 3a, 5a, and 17a shows the existence of a well-defined moisture band (mean relative humidity > 80%) from Vermont southwestward to Virginia. The axis of this moisture tongue lies to the west of the surface trough (Fig. 3a), ahead of the 500-mb trough (Fig. 5a), and within the area of cyclonic vorticity advection by the thermal wind (Fig. 6a), implying deep ascent and the generation of clouds and precipitation. The initialized RAFS moisture analysis (Fig. 17b), based on the same radiosonde data used to construct Fig. 17a, reveals that the model lower half of the troposphere (roughly the surface to 490 mb) is too dry in the vicinity of the coastal trough with mean relative humidities in the 50%–70% range. The 12-h RAFS forecast (Fig. 12c) is also too dry along the coastal trough with the area of mean relative humidity in excess of 70% concentrated too far north with the northern system shown in Fig. 14c. The 12-h RAFS forecast ascent center ($\sim -4 \times 10^{-3}$ hPa s^{-1}) over the Delmarva Peninsula immediately upstream of the weak cyclone along the New Jersey coast is thus acting on air that is too dry. A similar problem with the moisture analysis is seen for the 24-h RAFS forecast verifying 1200 UTC 3 October (Fig. 17d) because the moisture shield does not extend far enough southward along the coastal plain. On the basis of Fig. 17a, we are forced to conclude that, for this case at least, the RAFS analysis and initialization procedure was insensitive to the moisture information contained in the available data.

The representation of the wind field at 1200 UTC 3 October in the lowest sigma layer (Hoke et al. 1989), as operationally produced by RAFS, appears in Fig. 18. The mean elevation of this layer is approximately 200 m. The marine wind observations on which the RAFS automated analysis and initialization procedures are based are shown in Fig. 18d, along with selected wind reports from land stations. Similarly, the vector difference between the actual and initialized winds is superimposed over the initialized analysis in Fig. 18c for selected stations to facilitate comparison. (Caution: note the scale adjustment as the automated winds are plotted with a coarser resolution with one full and half barb denoting 10 and 5 m s^{-1}, respectively.) According to DiMego (1988) and Hoke et al. (1989), the RAFS automated analysis and initialization procedure disregards surface wind observations over land in favor of a geostrophic constraint, while retaining all available marine wind observations. Thus, surface wind analysis discrepancies in the RAFS may be more prevalent over continental areas, especially where there is significant ageostrophic flow.

While the RAFS analysis does change the west-northwesterly flow along the coast in the first guess to west-southwesterly, the initialization errors were not making the flow direction northerly enough over much

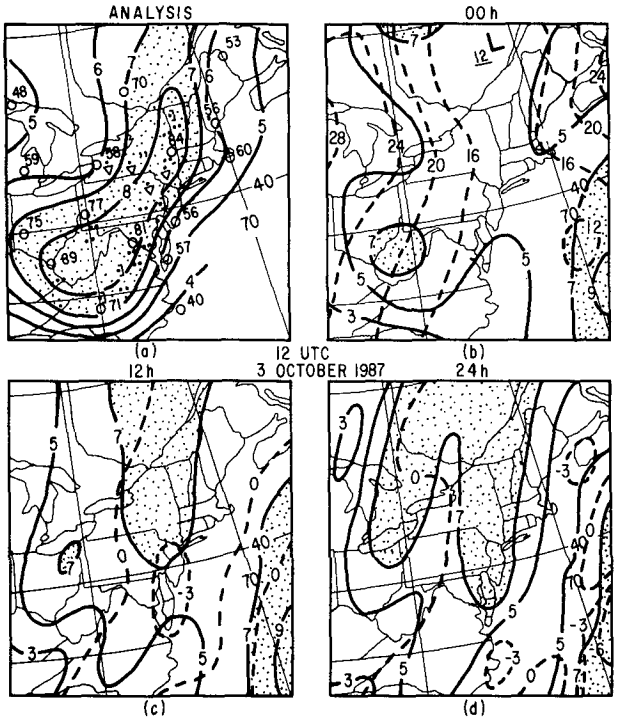

FIG. 17. (a) Mean surface–500-mb relative humidity (solid contours times 10%) with plotted radiosonde observations and surface precipitation reports for 1200 UTC 3 October 1987. Areas of mean relative humidity ≥ 70% are shown stippled. RAFS initialized (b), 12-h forecast (c), and 24-h forecast (d) mean relative humidity (solid contours times 10%) values ≥ 70% shown stippled. The 700-mb vertical motions ($\times 10^{-3}$ hPa s^{-1}) shown as dashed contours (zero contour and ascent only).

of New York, Pennsylvania, Delaware, Maryland, Virginia, North Carolina, and South Carolina; nor does it have the flow direction southerly enough along the coast in South Carolina, North Carolina, and Virginia. Similarly, the old offshore frontal boundary between 70° and 75°W is poorly resolved, particularly for the easterlies from near 35°N to east of BOS; in between the calm region from coastal New Jersey northward is not represented. As an example, the plot of the vector difference between the observed and initialized winds in Fig. 18c suggests that the relative vorticity in the coastal trough in the initialized analysis is underestimated. This can be confirmed by a computation of the relative vorticity along the observed trough axis in southern New Jersey and slightly farther west in the initialized analysis. An observed and initialized relative vorticity of 6.3×10^{-5} and 3.2×10^{-5} s^{-1}, respectively, is computed using a "two-delta" distance of 2° latitude (222 km). Even with an uncertainty allowance of 25% for this crude calculation we feel confident in asserting that the initialized wind analysis underestimates the relative vorticity along the coastal trough in the vicinity of where the incipient surface cyclone originates. Inspection of Fig. 3a confirms the existence of a local circulation center along the southern New Jersey coast, as there is no way to draw the isogons without having a singular point in this region. It is suggested that this circulation center is associated with the aforementioned vorticity trough. A similar calculation of the divergence from this analysis versus the RAFS analysis suggests values of -2.5 to -3.0×10^{-5} s^{-1} and $\sim -1.0 \times 10^{-5}$ s^{-1}, respectively, with somewhat greater uncertainty than for the relative humidity estimate.

The corresponding RAFS automated first guess and initialized surface (sigma = 1) temperature and specific-humidity analyses, and observed data are displayed in Fig. 19 for 1200 UTC 3 October. The difference fields in Figs. 19b and 19e speak for themselves. There is a systematic weakness in the initialized coastal temperature gradient from North Carolina southward, with the RAFS initialized temperature analysis seemingly oblivious to the existence of the Florida peninsula. Similarly, the RAFS initialized temperature gradient is underestimated across the Hudson Valley of New York, as temperatures are initialized too cold ahead of the trough. However, in the vicinity of the incipient disturbance in southern New Jersey, southward along the Delmarva Peninsula there is little systematic temperature error. Farther west, however, the initialized temperature gradient is again underestimated in the advancing cold air from southwestern Virginia to central Pennsylvania. Large negative temperature errors centered over the Canadian Maritimes are possibly a reflection of insufficient surface cooling over relatively cold water but appear to be inconsequential for our purposes. Lastly, the specific-humidity difference field is featureless along the coast with positive errors confined to the region south and east of the offshore frontal zone, particularly south of Bermuda. An exception is the 2 g kg^{-1} specific humidity underestimate northwest of the offshore warm front near 39°N,71°W. Air parcels drawn into the developing cyclonic circulation to the west from these regions are initialized too dry by a modest amount.

Figure 20 displays the RAFS automated wind analysis on the sigma (σ) = 3 surface (~897 mb or ~1000 m above the surface) for 1200 UTC 3 October. A comparison of the superimposed 900-mb rawinsonde observations across the eastern United States with the analysis reveals that the intensity of the trough near the coast is underestimated from North Carolina to Maryland in the analysis. For example, the reported 900-mb winds at IAD, ACY, and Wallops Island, Virginia (WAL), are 332° at 13 m s^{-1}, 223° at 8 m s^{-1}, and 233° at 9 m s^{-1}, respectively, in contrast to analyzed wind speeds of ~5 m s^{-1}. For a point centered over Chesapeake Bay directly east of IAD we compute a relative vorticity of 8.2×10^{-5} s^{-1} with a two-delta distance of 250 km. The same calculation from the analysis yields a relative vorticity of 2.6×10^{-5} s^{-1}. Although there is considerable uncertainty in these vorticity estimates, it is confidently concluded that the

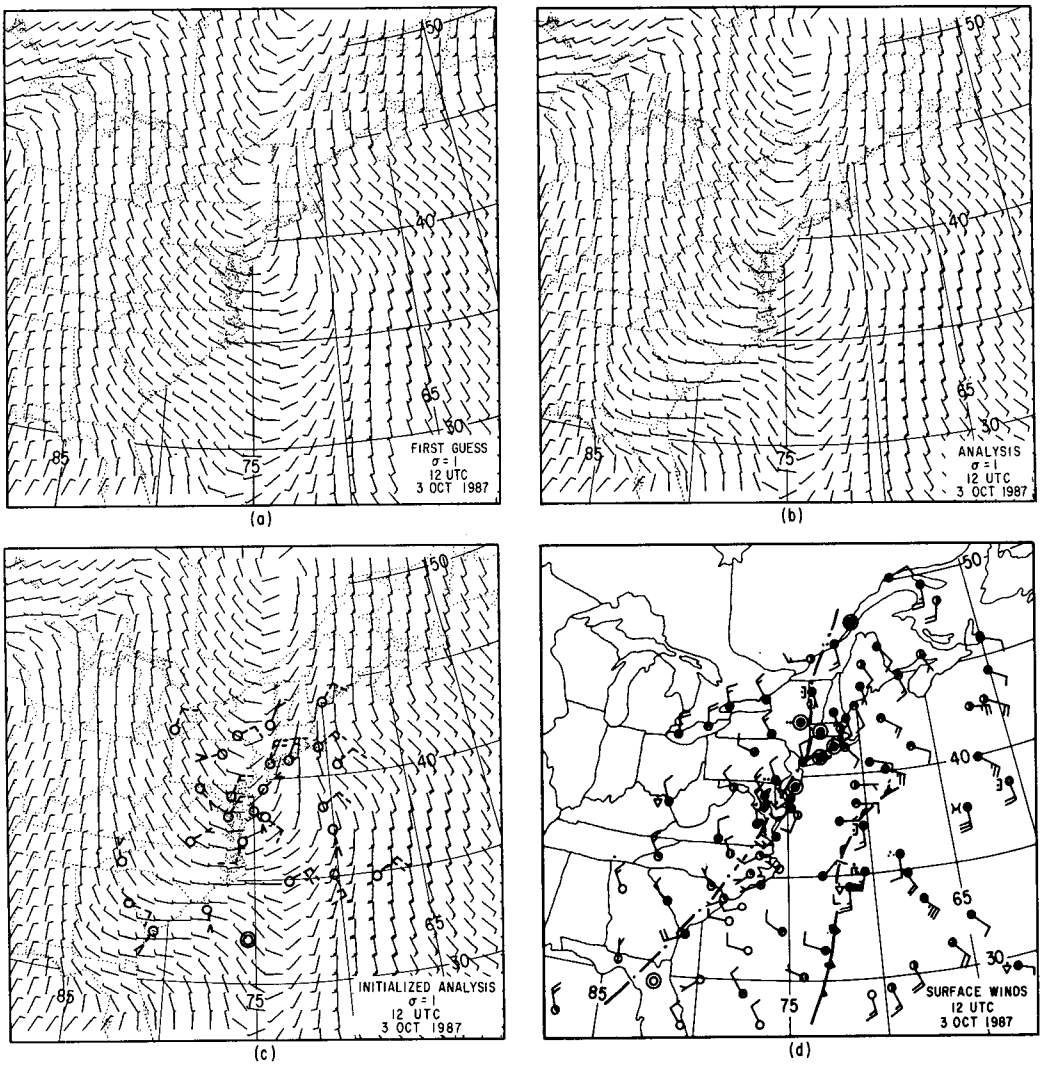

FIG. 18. RAFS 12-h first guess (a), analyzed (b), and initialized (c) wind field on the sigma = 1 surface (average pressure 982 mb and ~200 m above the surface) for 1200 UTC 3 October 1987. Observed winds and present weather are plotted in (d) according to the convention given in Fig. 3. Automated wind speed convention is one full barb (half barb) denotes 10 m s^{-1} (5 m s^{-1}) in (a), (b), and (c). Surface frontal and trough positions are shown according to standard convention. The vector difference between the actual and initialized winds is superimposed over the initialized analysis in (c). The vector wind difference is plotted in the format of Fig. 3.

relative vorticity is significantly underestimated in the lower troposphere in the vicinity of the incipient disturbance in the RAFS analysis for 1200 UTC 3 October.

For the same point east of IAD, a horizontal divergence of -2.9×10^{-5} s^{-1} at ~900 mb is estimated in contrast to a value of -1.0×10^{-5} s^{-1} from the RAFS analysis. The impact of these estimated vorticity and divergence differences on the production of cyclonic vorticity over a 24-h period can be significant. If we consider only the generation of vorticity by the full divergence term (retaining the absolute vorticity as a coefficient) and ignore horizontal vorticity advection and friction, then, for an initial surface–900-mb average absolute vorticity of 16×10^{-5} s^{-1} (7×10^{-10} s^{-1} relative vorticity), an absolute vorticity of 58.5 $\times 10^{-5}$ s^{-1} is computed 12 h later under the influence of a constant divergence field of -3.0×10^{-5} s^{-1}. A similar estimate based on the RAFS analyses would yield a 12-h absolute vorticity value of 18.5×10^{-5} s^{-1}, given a mean absolute vorticity of 12×10^{-5} s^{-1} and a mean divergence of -1.0×10^{-5} s^{-1}. Consequently, an initial absolute-vorticity underestimate of ~25% in the planetary boundary layer at 1200 UTC 3 October would lead to an almost 70% underestimate 12 h later if all other processes leading to vorticity change are ignored, an unlikely event but a useful upper-bound estimate.

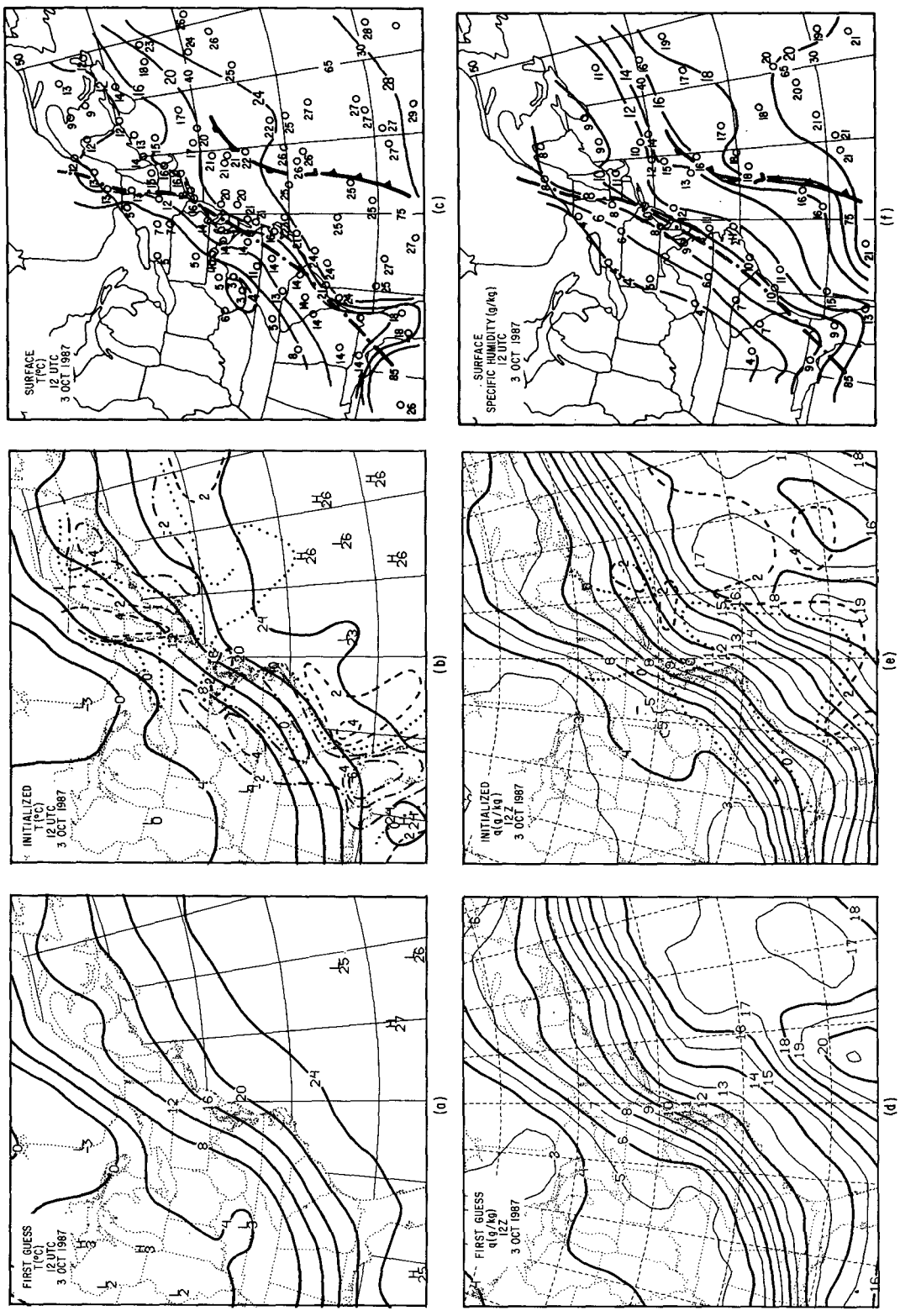

FIG. 19. First guess (a) and initialized (b) RAFS automated temperature analyses (°C) on the lowest sigma surface ($\sigma = 1$ approximately 200 m above the surface) for 1200 UTC 3 October 1987; (d), (e) as in (a) and (b) except for the specific humidity (g kg^{-1}). Actual observed surface temperatures (°C) and specific humidities (g kg^{-1}) are shown in (c) and (f), respectively, along with surface frontal and trough positions. The difference between the observed and initialized temperatures is contoured every 2°C in (b) with dashed (dash–dot) contours denoting positive (negative) values with the zero contour dotted. Similarly for the specific-humidity difference field in (e) with the contour interval every 2 g kg^{-1}.

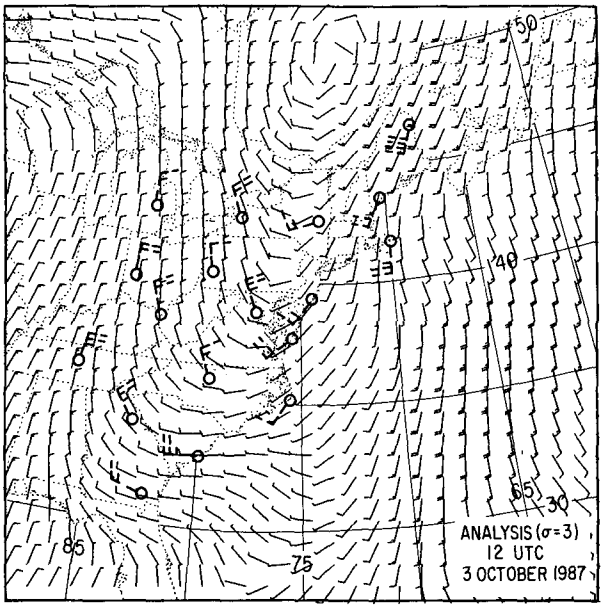

FIG. 20. RAFS automated wind analysis on the sigma = 3 surface (~897 mb or ~1000 m above the surface) for 1200 UTC 3 October 1987. Automated winds plotted according to the format of Fig. 18. Actual 900-mb wind observations are plotted in the format of Fig. 3 from radiosonde stations in the eastern United States.

6. Concluding discussion and summary

An unusual early-season snowstorm dumped in excess of 50 cm of unforecasted snow over portions of interior eastern New York and western New England on 4 October 1987. The storm was noteworthy because of an across-the-board NMC model failure to predict accurately the storm development off the mid-Atlantic coast and its associated precipitation. The storm central-pressure error and the displacement error for the 24-h RAFS forecast verifying 1200 UTC 4 October was 15 mb (underprediction) and 270 km (forecast too far to the east-southeast), respectively. Mullen and Smith (1990) carried out an analysis of errors in the operational RAFS forecasts for the 1987/88 winter season. Their statistics revealed root-mean-square mean sea level pressure and displacement errors of 5.66 mb and 268 km for 24-h forecasts based on a sample size of 995 storms. The model failure in this case represents an unusually big miss on central pressure (more than two root-mean-square errors on the low side) but not on final position at and after 1200 UTC 4 October. The model failures were puzzling because the storm life cycle followed well-known qualitative quasigeostrophic development principles as outlined by Sutcliffe (1947), Trenberth (1978), and Holton (1979), and even the flawed initialization showed a qualitatively favorable temperature gradient for development.

Our analyses revealed that the storm grew out of an area of enhanced vorticity along the New Jersey coast embedded in a slow-moving baroclinic zone that was crossing the Atlantic coast at 1200 UTC 3 October. The resulting vorticity maximum tracked southeastward and then eastward as cyclogenesis commenced with a closed 1004-mb low center evident by 0000 UTC 4 October approximately 300 km east of the Delaware coast. The initial southeastward and eastward storm drift can be viewed as a continuous redevelopment with no discrete new cyclone center. Rapid deepening occurred over the next 12-h period as the storm turned northeastward beneath an area of appreciable cyclonic vorticity advection by the thermal wind. A 991-mb low passed just west of BOS close to 1200 UTC 4 October with many locations reporting wind gusts in excess of 20–25 m s^{-1}. The storm satisfied the bomb criterion in terms of central pressure as discussed by Sanders and Gyakum (1980).

McGuire and Penn (1953) and Wexler et al. (1954) described a similar April snowfall event that occurred over eastern New England. They stressed the importance of atmospheric cooling by melting snow in a saturated environment to the production of a deep isothermal layer along the 0°C isotherm below cloud base. A similar process appeared to be acting in the October 1987 case. Cooling developed eastward across the Hudson Valley into western New England behind a weak trough passage. Precipitation falling into initially drier air enhanced the cooling, but it was insufficient to lower surface air temperatures to near freezing. (Note that when the air is dry below cloud base, sublimation of falling snow is much more effective than melting in producing cooling because the latent heat of sublimation is close to nine times larger than the latent heat of fusion. Widespread saturation in the present case before the onset of snow at the ground precludes an important role for sublimation.) It is also possible that ageostrophic cold advection associated with geostrophic frontogenesis across interior eastern New York and western New England in the lower troposphere, best seen at 850 mb, contributed to the formation of the cold pool.

Our conclusion that cooling by melting snow was a crucial factor in allowing snow to reach the surface is based on two factors. First, the ALB sounding data for 1200 UTC 4 October shows the existence of an ~200–300-m-thick 0°C isothermal layer just above the surface. The isothermal layer formed after a sustained 4–6-h period of heavy precipitation, averaging 4–6 mm h^{-1}, during which rain gradually mixed with ice pellets and wet snowflakes before changing over to all snow. Typically, the lowest surface temperatures (~0°C) were reported in the heavy-snow region. Second, an analysis of 74 local and regional climatological stations located within the snow area revealed minimum temperatures of ~0°C ± 1°C over a range of surface elevations from sea level to 800 m. This isothermal temperature dependence on elevation was attributed to atmospheric cooling by melting snow. Consequently, the storm becomes associated with a "self-

made" pool of cold air near 0°C that lies to the west of the actual surface cyclone center but almost directly beneath the upper-level vortex.

The typical 1000–500-mb thickness in the heavy snow region was 543 dam in contrast to the expected 540-dam climatological thickness value for the rain–snow transition regime. The end result of the cooling processes described above was the production of a wedge of cold air in the boundary layer resulting in a "warm snowstorm" in the terminology of Gedzelman and Lewis (1990). Above the snow region there was appreciable cyclonic vorticity advection by the thermal wind with the implied ascent mostly attributed to an upward increase of cyclonic vorticity advection, because the lower tropospheric thermal advection was very small. The absence of low-level warm-air advection over the snow region was crucial to the maintenance of the cold dome as relatively warm maritime air to the east (sea surface temperatures in early October were 12°–14°C) was prevented from reaching the area, eroding the cold dome, and changing snow to rain.

The NMC operational prediction models provided generally good prognoses of the movement and intensity of the upper-level short-wave trough and embedded vorticity maximum but poor prognoses of the track and strength of the corresponding sea level cyclone. This failure extended to all the forecast models at several lead times before the cyclogenesis event. The characteristic model error, shown for the RAFS forecasts in particular, was to take a considerably weaker cyclone up the Atlantic coast and 100–300 km farther offshore than observed during the rapidly intensifying stage. An inspection of the RAFS analysis and initialized fields for the lowest "sigma" layer (Phillips 1957) showed that during the incipient cyclogenesis stage the cyclone center was either not analyzed or placed too far east. As noted earlier, the RAFS analysis and initialization process routinely disregards surface wind observations over land in favor of a geostrophic constraint while retaining all available marine wind observations. It is conceivable that this approach could produce unrealistic initial vorticity and divergence fields in the lowest model sigma layers across a coastline, particularly in cold-air damming situations (Forbes et al. 1987; Bell and Bosart 1988), and strong cold advection situations when the surface wind directions are likely to be highly ageostrophic (downgradient) over land.

The evidence here is mixed. At the surface it appears that the RAFS initialized relative vorticity in the coastal New Jersey trough is roughly half that gleaned from the actual wind observations in the vicinity of the incipient disturbance. Near 900 mb, the RAFS-analyzed relative vorticity is only 30% of that deduced from radiosonde observations that straddle the coastal trough. A similar error is estimated for the divergence field. From this information we concluded that 1) the initial low-level vorticity maximum and convergence center embedded in the coastal baroclinic zone was underestimated in the RAFS analysis and initialized fields, and 2) the RAFS analysis and initialization procedure proved to be too insensitive to the actual surface land and marine wind observations as well as selected lower-tropospheric rawindsonde observations in the vicinity of the coastal trough at the time (1200 UTC 3 October) of the initial cyclogenesis.

Another major model error was the RAFS underprediction of mean relative humidity in the lower half of the troposphere in the incipient storm environment at 1200 UTC 3 October. Likewise, the relative humidities were not initialized wet enough in comparison to observation in a broad area immediately upstream of the developing cyclone. This point is reinforced by observations made by the second author aboard his sailing craft, the *Stillwater,* along the New Jersey coast. The log book on the *Stillwater* reads at 1600 UTC 3 October "40.65°N, 74.04°W, wind north at 11 knots, breaks in the overcast with middle and high cloud present." At 1810 UTC the log reads "40.49°N, 73.94°W, wind north at 16 knots, broken skies with swelling cumulus over land and cirrus above." By 2000 UTC it was "more ominous at 40.32°N, 72.95°W with a north wind of 26 knots." At 2200 UTC the log reports "40.06°N, 74.02°W, wind 346° at 36 knots. Squalls. Gusts 10 knots higher. Thunder. Solid overcast with violent showers superposed." The first lightning flashes were noticed offshore and then to the south-southwest over land. By 0000 UTC 4 October the log reveals "39.80°N, 74.06°W (near ACY when the Showalter index based on an 850-mb temperature of 7°C in saturated air is ~0 in Fig. 5), light rain with occasional moderate rain showers. Squally." These observations are consistent with an atmosphere rapidly moistening after 1200 UTC 3 October and developing pockets of positive convective available potential energy. This interpretation is consistent with our mean-layer relative humidity analysis shown in Fig. 17a for 1200 UTC 3 October. Thus, it would appear that the NMC models were operating on too dry an atmosphere, and the positive feedback process between ascent and latent heat release leading to cyclonic vorticity growth in an atmosphere of near neutrality was curtailed.

Our initial working hypothesis was that the RAFS model, deprived of adequate knowledge about the strength of the initial coastal vorticity maximum and associated thermal field, locked on to the old baroclinic zone farther offshore and produced a weaker storm tracking northeastward well east of the coast on the fringe of the major region of cyclonic vorticity advection by the thermal wind aloft. This hypothesis had to be abandoned when it became clear from an inspection of the RAFS analysis and initialized fields that, at the time of incipient cyclogenesis over coastal southern New Jersey, the surface circulation along the offshore baroclinic zone was underestimated as well. Similarly, although the RAFS initialized baroclinicity was un-

derestimated along much of the coastal trough, this was not the case in the vicinity of the initial development. While we can not claim any quantitative understanding of the reasons for the failure of the RAFS model to predict this case of explosive cyclogenesis, the available qualitative evidence points to an inadequate representation of boundary-layer vorticity and divergence in the coastal baroclinic zone and mean relative humidity in the lower half of the troposphere as major contributors to the poor forecasts.

We also note that the MRF and LFM models suffered from the same forecast problems, but we lacked access to the gridded analyzed and initialized fields for these models to perform the same kind of analysis that we did for the RAFS model. Certainly, the NMC models have proven themselves capable of successfully simulating explosive cyclogenesis in recent years (see, e.g., Sanders 1986, 1987b), a spectacular recent example is the ERICA (Experiment on Rapidly Intensifying Cyclones over the Atlantic) western Atlantic bomb of 4 January 1989. Also, the poor model forecasts cannot be attributed to horizontal-resolution problems. An experimental "D-grid" version of the RAFS (~40-km resolution) model was initialized and run from 0000 UTC 3 October. Although, some improvement was noted, the model forecast cyclone was too weak, too fast, and too far offshore, with the result that precipitation over land was still severely underestimated. As the RAFS model history tapes were not saved for this experimental run, we could not obtain access to any of the gridded analysis and forecast fields for further analysis.

In conclusion, we reiterate our belief that there was nothing really unusual about the cyclone that buried portions of the interior northeastern United States with more than 50 cm of snow on 4 October. Storm development can be well understood from simple qualitative quasigeostrophic reasoning, and indeed, the NMC prediction models accurately predicted the track, timing, and intensity of the 500-mb vorticity maximum that triggered cyclogenesis. The cyclone spinup process associated with the approach of the updraft region ahead of the mobile trough aloft was rendered relatively ineffective because 1) the ambient vorticity and divergence in the lower troposphere along the coastal trough were underestimated in the model analysis and initialization procedure, and 2) the ascending region in the incipient storm environment was initialized too dry.

The misrepresentation of the lower-tropospheric vorticity and moisture fields imply an underestimation of the strength of the positive potential vorticity (PV) anomaly along the coastal baroclinic zone in the incipient storm environment. According to Hoskins et al. (1985), cyclogenesis is enhanced when an upper-level PV anomaly approaches a lower-level PV anomaly. This results in a positive feedback process between the two anomalies, leading to cyclonic vorticity generation throughout the troposphere. Our results imply that a lower-level PV anomaly was underestimated in the model initial state and that this misrepresentation probably contributed to the poor cyclogenesis forecasts. In reality, however, the very sharp baroclinic zone created by the juxtaposition of a dome of cold continental air, reinforced by cooling associated with melting snow, and relatively warm marine air (it was just past the time of climatologically warmest sea surface temperatures) created ample opportunity for air parcels to ascend along uplifted isentropic surfaces marking the cold dome beneath the advancing PV anomaly aloft, thus, sustaining locally vigorous ascent and heavy precipitation.

Acknowledgments. The authors thank Dr. Eric Rogers for providing us with access to the NMC RAFS first guess, analyzed, and initialized fields. The first author appreciated the opportunity to share scientific discussions and "war stories" about this event with Dr. Stanley Gedzelman. Research support was provided by NSF Grant ATM8805550 and ONR Contracts N00014-87-K-0209 and N00014-85-C-0785. The manuscript was prepared by Ms. Celeste Iovinella, and the figures were drafted by Ms. Marilyn Peacock.

REFERENCES

Bell, G. D., and L. F. Bosart, 1988: Appalachian cold-air damming. *Mon. Wea. Rev.*, **116,** 137–161.

Caplan, P. M., and G. H. White, 1989: Performance of the National Meteorological Center's medium-range model. *Wea. Forecasting,* **4,** 391–400.

Carter, G. M., J. P. Dallavalle and H. R. Glahn, 1989: Statistical forecasts based on the National Meteorological Center's numerical weather prediction system. *Wea. Forecasting,* **4,** 401–412.

DiMego, G. J., 1988: The National Meteorological Center regional analysis system. *Mon. Wea. Rev.*, **116,** 977–1000.

Forbes, G. S., R. A. Anthes and D. W. Thomson, 1987: Synoptic and mesoscale aspects of an Appalachian ice storm associated with cold-air damming. *Mon. Wea. Rev.*, **115,** 564–591.

Gedzelman, S. D., and E. Lewis, 1990: Warm snowstorms: A forecasters dilemma. *Weatherwise,* **43,** 265–270.

Gerrity, J., 1977: The LFM model-1976: A documentation—NOAA Tech. Memor. NWS NMC-60 (NTIS PB-279-419), 68 pp.

Glann, H. R., and D. A. Lowry, 1972: The use of model output statistics (MOS) in objective weather forecasting. *J. Appl. Meteor.*, **11,** 1203–1211.

Hoke, J. E., N. A. Phillips, G. J. DiMego, J. J. Tuccillo and J. Sela, 1989: The regional analysis and forecast system of the National Meteorological Center. *Wea. Forecasting,* **4,** 323–334.

Holton, J. R., 1979: *An Introduction to Dynamic Meteorology.* Academic Press, 391 pp.

Homan, J., and L. W. Uccellini, 1987: Winter forecast problems associated with light to moderate snow events in the mid-Atlantic states on 14 and 22 February 1986. *Wea. Forecasting,* **2,** 206–228.

Hoskins, B. J., M. E. McIntyre and A. W. Robertson, 1985: On the use and significance of isentropic potential vorticity maps. *Quart. J. Roy. Meteor. Soc.*, **111,** 877–946.

Kanamitsu, M., 1989: Description of the NMC global data assimilation and forecast system. *Wea. Forecasting,* **4,** 335–342.

Lin, C. A., and R. E. Stewart, 1986: Mesoscale circulations initiated by melting snow. *J. Geophys. Res.*, **91**, 13 299–13 302.

Ludlum, D. M., 1966: *Early American Winters I 1604–1820.* Amer. Meteor. Soc. 283 pp.

——, 1968: *Early American Winters II 1821–1870.* Amer. Meteor. Soc., 257 pp.

Matsuo, T., and Y. Sasyo, 1981a: Empirical formula for the melting rate of snowflakes. *J. Meteor. Soc. Japan*, **59**, 1–9.

——, and Y. Sasyo, 1981b: Melting of snowflakes below freezing level in the atmosphere. *J. Meteor. Soc. Japan*, **59**, 10–25.

——, and ——, 1981c: Nonmelting phenomena of snowflakes observed in subsaturated air below freezing level. *J. Meteor. Soc. Japan*, **59**, 26–32.

McGuire, J., and S. Penn, 1953: Why did it snow at Boston in April? *Weatherwise*, **6**, 78–81.

Mullen, S. L., and B. B. Smith, 1990: An analysis of sea-level cyclone errors in NMC's nested grid model (NGM) during the 1987–88 winter season. *Wea. Forecasting*, **5**, 433–447.

NOAA, 1987: *Oceanographic Monthly Summary.* United States Department of Commerce, NOAA, National Weather Service, 23 pp.

Phillips, N. A., 1957: A coordinate system having some special advantages for numerical forecasting. *J. Meteor.*, **14**, 184–185.

Sanders, F., 1986: Explosive cyclogenesis over the west-central North Atlantic Ocean, 1981–84. Part II: Evaluation of LFM model performance. *Mon. Wea. Rev.*, **114**, 2207–2218.

——, 1987a: A study of 500 mb vorticity maxima crossing the East Coast of North American and associated surface cyclogenesis. *Wea. Forecasting*, **2**, 70–83.

——, 1987b: Skill of NMC operational dynamical models in the prediction of explosive cyclogenesis. *Wea. Forecasting*, **2**, 322–336.

——, and J. R. Gyakum, 1980: Synoptic–dynamic climatology of the "bomb". *Mon. Wea. Rev.*, **108**, 1589–1606.

Sela, J. R., 1980: Spectral modeling at NMC. *Mon. Wea. Rev.*, **108**, 1279–1292.

Stewart, R. E., 1984: Deep 0°C isothermal layers within precipitation bands over southern Ontario. *J. Geophys. Res.*, **89**, 2567–2572.

——, 1985: Precipitation types in winter storms. *Pure Appl. Geophys.*, **123**, 597–609.

——, and P. King, 1987a: Freezing precipitation in winter storms. *Mon. Wea. Rev.*, **115**, 1270–1279.

——, and ——, 1987b: Rain–snow boundaries over southern Ontario. *Mon. Wea. Rev.*, **115**, 1894–1907.

——, J. D. Marwitz, J. C. Pace and R. E. Carbone, 1984: Characteristics through the melting layer of stratiform clouds. *J. Atmos. Sci.*, **41**, 3227–3237.

Sutcliffe, R. C., 1947: A contribution to the problem of development. *Quart. J. Roy. Meteor. Soc.*, **73**, 370–383.

Szeto, K. K., C. A. Lin and R. E. Stewart, 1988a: Mesoscale circulations forced by melting snow. Part I: Basic simulations and dynamics. *J. Atmos. Sci.*, **45**, 1629–1641.

——, R. E. Stewart and C. A. Lin, 1988b: Mesoscale circulations forced by melting snow. Part II: Application to meteorological features. *J. Atmos. Sci.*, **45**, 1642–1650.

Trenberth, K. E., 1978: On the interpretation of the diagnostic quasi-geostrophic omega equation. *Mon. Wea. Rev.*, **106**, 131–137.

Wexler, R., R. J. Reed and J. Honig, 1954: Atmospheric cooling by melting snow. *Bull. Amer. Meteor. Soc.*, **35**, 48–51.